

# **BONDING AND CRACKING BEHAVIOR AND RELATED PROPERTIES OF CEMENTITIOUS GROUT IN AN INTERMEDIATE-SCALE GROUT MONOLITH**

*Prepared for*

**U.S. Nuclear Regulatory Commission  
Contract NRC-02-07-006**

*Prepared by*

**Cynthia L. Dinwiddie<sup>1</sup>  
Gary R. Walter<sup>1</sup>  
Glenn Light<sup>2</sup>  
Steven Winterberg<sup>2</sup>  
Danielle Wyrick<sup>1</sup>  
Darrell Sims<sup>1</sup>  
Kevin Smart<sup>1</sup>**

**<sup>1</sup>Department of Earth, Material, and Planetary Sciences  
Southwest Research Institute<sup>®</sup>, San Antonio, Texas**

**<sup>2</sup>Department of Sensor Systems and NDE Technology  
Southwest Research Institute<sup>®</sup>, San Antonio, Texas**

**Center for Nuclear Waste Regulatory Analyses  
San Antonio, Texas**

**September 2011**

## PREVIOUS REPORTS IN SERIES

Number	Name	Date Issued
14003.01.007.222	Conceptual Design for Small-Scale Grout Monolith Tests	April 2008
14003.01.007.305	Mesoscale Grout Monolith Experiments: Results and Recommendations	May 2009
14003.01.007.445	Intermediate-Scale Grout Monolith and Additional Mesoscale Grout Monolith Experiments: Results and Recommendations—Status Report	September 2010

# CONTENTS

Section	Page
FIGURES .....	v
TABLES .....	vii
EXECUTIVE SUMMARY .....	viii
ACKNOWLEDGMENTS .....	xvi
1 BACKGROUND AND SCOPE OF REPORT .....	1-1
2 TESTING OF BOND BETWEEN GROUT AND TANK WALL.....	2-1
2.1 Conceptual Solution Using Ultrasonic Inspection.....	2-1
2.1.1 Theory .....	2-1
2.1.2 Laboratory Tests and Data Collected From Mesoscale Drum Grout Specimens .....	2-2
2.2 Ultrasonic and Coin-Tap Test Data Acquisition From Intermediate-Scale Grout Monolith and Results .....	2-4
2.3 Destructive Testing Results.....	2-5
2.4 Surface Morphology of Excised Tank Wall Sections Using Dynamic Structured Light .....	2-8
2.4.1 Method.....	2-8
2.4.2 Results and Observations.....	2-12
2.5 Conclusions.....	2-12
3 WALL AND CORE SAMPLING, INSPECTION, AND DESCRIPTION.....	3-1
3.1 Wet-Coring and Water-Flow Observations.....	3-1
3.2 Epoxy Application and Observations.....	3-6
3.3 Core Observations .....	3-7
3.3.1 Corehole 7 .....	3-8
3.3.2 Corehole 8 .....	3-8
3.3.3 Corehole 9 .....	3-10
3.4 Wall Observations .....	3-10
3.4.1 Section One .....	3-12
3.4.2 Section Three .....	3-13
3.4.3 Conclusions and Recommendations .....	3-14
4 SURFACE CRACK CHARACTERIZATION.....	4-1
5 REVIEW OF CRACKING MECHANISMS IN GROUT MONOLITHS AND INTERPRETATION OF CRACKS OBSERVED IN GROUT SPECIMENS .....	5-1
5.1 Plastic Shrinkage, Plastic Settlement, and Presetting Cracking.....	5-1
5.2 Hydration and Drying Shrinkage Cracking .....	5-1
5.3 Thermomechanical Cracking.....	5-2
5.4 Other Mechanical Stress-Induced Cracking .....	5-2
5.5 Interpretation of Cracks Observed in Grout Specimens .....	5-3
5.5.1 Horizontal Cracks .....	5-3
5.5.2 Shallow, Relatively Large-Aperture, Subvertical Cracks, and Matrix Color .....	5-3
5.5.3 Narrow-Aperture, Linear, Vertical Cracks .....	5-4

## CONTENTS (continued)

Section		Page
	5.5.4 Cracks Induced by Coring Operations and Possibly Also by Settlement.....	5-5
	5.5.5 Annuli Surrounding Internal Fixtures and Grout–Tank Wall Debonds ....	5-5
6	MATHEMATICAL MODELS FOR PREDICTING CRACKING .....	6-1
7	POTENTIAL SIGNIFICANCE OF GROUT DEBONDING AND CRACKING FOR NDAA GROUT MONOLITHS .....	7-1
	7.1 Potential for Grout Debonding .....	7-1
	7.2 Potential for Plastic Shrinkage and Settlement and Presetting Cracking, and for Hydration and Drying Shrinkage Cracking .....	7-2
	7.3 Potential for Thermomechanical Stress Cracking .....	7-3
	7.4 Potential for Other Mechanical Stress Cracking.....	7-3
8	SUMMARY AND RECOMMENDATIONS .....	8-1
	8.1 Observations and Findings Related to the Intermediate-Scale Grout Monolith .....	8-1
	8.2 Summary of Literature Review of Cracking Mechanisms.....	8-3
	8.3 Future Work and Recommendations.....	8-5
9	REFERENCES.....	9-1

## FIGURES

Figure		Page
2-1	Illustration of the Reflection of Ultrasonic Waves From Steel–Air and Steel–Grout Interfaces .....	2-2
2-2	Illustration of the Expected Ultrasonic Signal Amplitude Data .....	2-3
2-3	Ultrasonic and Coin-Tap Test Results for Each Lift Within Five Drum Grout Specimens.....	2-3
2-4	Ultrasonic Signal Amplitude Data Collected From Drum Grout Specimens.....	2-4
2-5	Illustration of the Section One Grid on the Tank Wall .....	2-5
2-6	Illustration of the Section Two Grid on the Tank Wall .....	2-6
2-7	Illustration of the Section Three Grid on the Tank Wall.....	2-6
2-8	Illustration of the Section Four Grid on the Tank Wall.....	2-7
2-9	Photographs of the Grout Surface Adjacent to the Removed Tank Wall Within the Section One Grid.....	2-7
2-10	Photograph of the Grout Surface Adjacent to the Removed Tank Wall Within the Section Three Grid .....	2-8
2-11	Photograph of Section One Grout Near the Base of Lift 3 .....	2-9
2-12	Photograph of Section One Grout at the Top of Lift 2 .....	2-9
2-13	Photograph of Section Three Grout .....	2-10
2-14	Photograph of Section Three Grout .....	2-10
2-15	Photograph of Section Three Grout .....	2-11
2-16	Photograph of Section Three Grout .....	2-11
2-17(a)	Dynamic Structured Light Data Presented as Digital Shaded Relief of the Upper Lift Exposed on the Interior Surface of the Section One Steel Tank Wall .....	2-13
2-17(b)	Digital Photograph of the Mirror Image Area Shown in Figure 2-11 and the Area Shown in Figure 2-17(a).....	2-14
2-18(a)	Digital Shaded Relief Mosaic of a Portion of the Interior Surface of the Section Three Wall.....	2-15
2-18(b)	Digital Photomosaic of Area Shown in Figure 2-18(a) .....	2-16
2-19(a)	Digital Shaded Relief Mosaic of a Portion of the Interior Surface of the Section Three Steel Tank Wall.....	2-17
2-19(b)	Digital Photomosaic of Area Shown in Figure 2-19(a) .....	2-18
3-1	Photomosaic of Surface of the Intermediate-Scale Grout Monolith .....	3-2
3-2	Water Breakthrough at Exposed Grout Surfaces Following Wet-Coring Operations on April 21, 2011.....	3-3
3-3(a)	Section One Water Breakthrough on May 23, 2011, Following Wet-Overcoring Operations at Corehole 7 .....	3-4
3-3(b)	Section Three Water Breakthrough on May 23, 2011, Following Wet-Overcoring Operations at Coreholes 8 and 9 .....	3-5
3-4	Overcore 7 .....	3-6
3-5(a)	Photograph of Overcores 7 and 8 Illustrates the Rubbleized Zone of Grout and Blue Epoxy That Comprise the Top of Overcore 8 .....	3-9
3-5(b)	View Into Corehole 8.....	3-9
3-6	Intact Section of Overcore 8 From Base to Height of 32 cm [12.6 in] .....	3-9
3-7	Overcore 9 .....	3-11

## FIGURES (continued)

Figure		Page
3-8	Intermediate-Scale Grout Monolith as Photographed in Cross Section .....	3-12
3-9	Crack Systems Developed at Intermediate-Scale Grout Monolith's Wall Exposures as of 19 May 2011 .....	3-13
4-1	Photograph of Scaffold-Mounted Laser Scanner Used To Measure Surface Topography.....	4-2
4-2	Photomosaic of the Intermediate-Scale Grout Monolith With Crack Distribution Patterns Traced and Coreholes 1–6 Shown .....	4-3
4-3	Photomosaic of the Intermediate-Scale Grout Monolith Draped With Aperture Values Measured Along its Surface Cracks .....	4-4
4-4	Photomosaic of the Intermediate-Scale Grout Monolith With Measurement Grid Used to Determine the Surface Crack Frequency Distribution.....	4-5
4-5	Photomosaic of the Intermediate-Scale Grout Monolith Draped With a Topographic Map .....	4-6
4-6	A Slope Map of the Intermediate-Scale Grout Monolith With Crack Distribution Patterns.....	4-7

## TABLE

Table		Page
1-1	Summary of Grout Batch Quantities, Flow Measurements, and Weather Conditions During Pours .....	1-3
5-1	Cracking Mechanism Types, Causes, Morphology, and Timing .....	5-1

## EXECUTIVE SUMMARY

Under Section 3116 of the Ronald W. Reagan National Defense Authorization Act of Fiscal Year 2005 (NDAA), the U.S. Nuclear Regulatory Commission (NRC) is responsible for consulting with the U.S. Department of Energy (DOE) on the DOE waste determinations for certain waste tanks and vaults at the Savannah River Site and Idaho National Laboratory, and for monitoring disposal actions taken by DOE pursuant to NDAA Section 3116, Subsection (a)(3), Subparagraphs (A) and (B) for the purpose of assessing compliance with the performance objectives of 10 CFR Part 61, Subpart C. NRC staff use information from independent analyses that support their consultation responsibilities under the NDAA.

Under the provisions of this Act, DOE stabilizes waste tanks and vaults with cementitious materials, such as grout. To support NRC, the Center for Nuclear Waste Regulatory Analyses (CNWRA<sup>®</sup>) has been tasked to provide mechanistic information on the physical and chemical degradation of cementitious waste forms that are used for the isolation and containment of radioactive wastes and to evaluate the potential for radionuclide bypass of the engineered barriers via preferential or fast pathways.

To establish a base-level understanding of the potential for fast flow pathways to form within grout soon after it is emplaced in a waste tank, CNWRA staff developed the intermediate-scale grout monolith specimen at Southwest Research Institute<sup>®</sup> (SwRI<sup>®</sup>) facilities in San Antonio, Texas, as an analog to grouted tanks at NDAA facilities (Walter, et al., 2009, 2010). In fiscal year 2011, CNWRA investigated the bonding and cracking behavior and related properties of cementitious grout in the intermediate-scale grout monolith. This grout is similar to reducing grout that may be used to stabilize NDAA waste tanks. These investigations included

- Nondestructive evaluation of the presence or lack of air gaps between the grout mass and the tank liner using ultrasonic testing and coin-tap testing
- Destructive evaluation of the interface between the grout and two discrete sections removed from the tank wall
- Observations of water breakthrough patterns on the exposed grout wall following water injection during wet-coring operations
- Measurements and descriptions of the two exposed grout wall sections and three extracted cores, including the presence and characteristics of horizontal partings and vertical-to-subvertical cracks
- High-resolution laser measurements of the surface topography of the grout monolith and detailed mapping and geographic-information-systems-based analysis of variable crack apertures, crack frequencies, and crack types on its surface
- Synthesis of literature describing cracking mechanisms in large concrete infrastructure and interpretation of observed grout monolith cracks in terms of known cracking mechanisms
- A brief literature review of numerical modeling work undertaken by others that might form a foundation from which to begin NDAA-focused modeling to better understand key factors affecting the formation of cracks in grout monoliths

- Interpretation of the potential significances of bonding and cracking for NDAA grout monoliths

The intent of the investigations was to gain insight into risk-significant aspects of grout behavior and properties that affect its performance. Due to differences in the formulation of the grout used in this investigation, and differences in the conditions of emplacement and curing, the findings reported here may not represent the behavior and properties of grouts used in actual closure of NDAA tanks. We are unaware of equivalent studies performed with the material components of NDAA tank grouts, nor have we received final recipes for grouts intended to be used for tank closure at the Savannah River Site, South Carolina. Because the U.S. Department of Energy has not supplied grout monolith performance information of an equivalent nature, NRC staff will likely use the independently acquired information contained within this and predecessor reports to support their consultation responsibilities for non-high-level, waste-incident-to-reprocessing determinations and their monitoring responsibilities for subsequent actions taken under the NDAA.

Ultrasonic and coin-tap nondestructive testing methods were used to investigate the bond between the grout and the tank liner (i.e., the wall) of the intermediate-scale grout monolith. Based upon comparison of the ultrasonic inspection results with the destructive testing of two sections of the intermediate-scale grout monolith's tank wall, it appears that the zero degree, longitudinal ultrasonic technique provided a good means to determine whether the interface between the grout and the tank wall was affected by the presence of an air gap. While the presence of an air gap is strongly suggestive of a debonded condition, the lack of an air gap does not conclusively prove that a bond exists between the grout and the tank liner or wall. Because the coin-tap test is only capable of identifying larger voids, this test method did not prove reliable for detecting small air gaps that were positively identified by the ultrasonic method, but it was useful for identifying the presence of near-surface air gaps located behind near-vertical cracks at the grout-tank wall interface.

Dynamic structured light imaging and high-resolution photographic methods were used to investigate the grout residue that remained adhered to two destructively removed sections of the tank wall. Results provide insight into the nature of the interface between tank wall and grout. Observations indicate that bonding of grout to tank wall is not uniform. As grout was emplaced in the intermediate-scale grout monolith, grout commonly spattered onto the tank liner above the existing grout level and during later pours was covered over by the emplaced bulk grout mass. Destructive removal of two tank wall sections illustrated that these early cured grout spatters sometimes adhere well to the tank wall and sometimes remain with the grout mass. Although spatter can adhere to the tank wall, the bulk grout mass may not adhere well to the spatter, with the result that a vertical discontinuity exists within a few millimeters of the tank wall. Though not a crack *sensu stricto*, the discontinuity may appear and act as a crack. Because grout emplaced within the monolith was not vibrated to enhance compaction and leveling and to eliminate the presence of air bubbles, the presence of grout spatter on tank walls leads to additional pore space surrounding each spatter because freshly poured bulk grout tends to not flow into all available void space surrounding early-cured grout spatters.

Destructive removal of the two tank wall sections changed the stress state within the monolith, causing existing cracks to evolve and new cracks to develop. Grout within lower lifts tends to be smoother than grout within the uppermost lift, which is attributed to the role played by overburden pressure that tends to compress voids, vesicles, vugs, and air bubbles in the lower lifts of grout. Smoother grout may correspond to more favorable permeabilities: the results of gas injection testing (Walter, et al., 2010) indicated a decrease in permeability with depth.

Interface quality between the three lifts was variable, with grout at an interface either tending to remain with the grout mass or tending to adhere to the removed tank liner sections.

Observations of epoxy uptake by crack systems and wet-coring water that seeped from the exposed sides of the intermediate-scale grout monolith indicate the presence of an extensive network of permeable pathways through the specimen. A horizontal parting or interface between two grout lifts played a significant role in conducting water from cored holes to the perimeter of the monolith. Water in the wet-cored holes likely ponded to at least this height, providing a direct source of water to this lift interface. Although this interface was highly conductive to water, it was not conductive to epoxy; epoxy was not observed to have flowed into the gaps between grout lifts. Permeable pathways like these were not observed in smaller scale specimens (Walter, et al., 2009, 2010), perhaps indicating that samples of sufficient size are needed to generate such features.

Features revealed through extraction of cores ranged from matrix color variations to vug sizes, crack distributions, apertures, and trace lengths. All cores had a matrix color change from light tan nearest the monolith surface to gray at depths. This color change may be strongly associated with the evaporation zone where early plastic shrinkage cracking and later hydration and drying shrinkage cracking occur. The color change is inferred to be related to weathering of the grout in close association with the atmosphere including such processes as oxidation, carbonation, and capillarity migration of dissolved constituents—an interpretation supported by similar light tan colors at deeper depths surrounding cracks that are open to the atmosphere. Excess porosity is present in the form of vesicles and vugs because the grout was not vibrated subsequent to emplacement. The three extracted cores provide evidence that various material components or grout ingredients were incompletely mixed at the batch plant or during delivery to the site, leaving some vugs partly filled with friable particulate matter. Incomplete mixing could result from the lack of coarse aggregate in the grout recipe, which would otherwise contribute to mixing. CNWRA staff do not have information regarding how common it is for grout components to be incompletely mixed by batch plant operators, but based upon our experience mixing small batches for mesoscale grout monoliths, incomplete mixing of material into the grout gel is not surprising. Walter, et al. (2009) specifically mentioned that SRS Alternative 1 Grout was difficult to mix even in small batches because fines tended to ball-up in dry clods, like dry ingredients will within a cake batter. Cracks are sometimes observed to penetrate relatively soft clasts instead of forming around clast edges. Horizontal crack intensity, as estimated from vertical cores, is four to seven cracks per meter [one to two cracks per foot]. Vertical and subvertical cracks, however, are undersampled by vertical core and are best understood at this time from an analysis of cracks intersecting the grout surface.

Staff further characterized the 218 cracks exposed on the surface of the intermediate-scale grout monolith by mapping their locations and variable apertures (see Section 4 photographs). Cracks are distributed in fairly distinct sets, including (i) radial to the monolith, (ii) roughly perpendicular to lobe flow fronts, (iii) two *en echelon* cracks that nearly bisect the monolith into equal halves, and (iv) a few cracks/crack families concentric to the monolith edge. Crack aperture varied from <0.5 to 8 mm [<0.02 to 0.31 in], with variation in aperture along crack length. Aperture values of at least 4 mm [0.16 in] were found in each quadrant of the monolith. Crack frequency, computed for 12 equal areas on the surface of the monolith, ranged from 1 to 26 cracks per square meter [ $9.3 \times 10^{-2}$  to 2.4 cracks per sq. ft]. Crack frequency is highest within the mounded grout flow lobes. The center of the grout monolith, where grout was preferentially pumped, is 21.9 cm [8.6 in] higher than the lowest point in the northeast quadrant of the tank, and topography is correlated to crack distribution, with higher crack frequency in areas of higher topography. Many cracks terminate at or near the edge of mounded grout

flow lobes. Shallow, wide-aperture, subvertical cracks were observed to form at the surface of all three lifts of the intermediate-scale grout monolith. These cracks connect with horizontal partings and vertical throughgoing cracks to form a crack network throughout the monolith.

Grout cracking mechanisms identified through a literature review are summarized in Table ES–1, along with causative factors, morphology (where known) and timing of formation. Concrete literature is vague regarding measurable crack characteristics that would allow definitive determination of cracking mechanisms, and some cracks may reflect a combined response to more than one cracking mechanism.

Plastic shrinkage, plastic settlement, and presetting cracks are related to contraction due to early water loss (i.e., evaporation from a free surface). Hydration and drying shrinkage occurs later during the curing process by incorporation of water molecules into the mineral structure of the cement paste and by loss of water to evaporation at the concrete surface. Drying shrinkage is commonly of minor importance to formation of cracks in massive concrete infrastructure (Springenschmid, 1994), but this may be due to common use of vibration or other compaction mechanisms that have no bearing on NDAA tank closure. Plastic shrinkage cracking, plastic settlement cracking, presetting cracking, and hydration and drying shrinkage cracking are interpreted to have played a major role in the development of numerous, relatively shallow but wide-aperture subvertical cracks in multiple lifts within the intermediate-scale grout monolith. These cracks formed in a near 100 percent relative humidity environment because the monolith was covered with an impervious plastic sheet for approximately 1 month after the final pour of the final lift was emplaced. High humidity is also expected within NDAA tanks during early curing.

Heat of hydration and resultant large temperature gradients within massive concrete infrastructure (both reinforced and unreinforced) are of primary importance to restraint stresses and the formation of cracks (Springenschmid, 1994), but this observation may not directly apply to the grout formulations being considered for NDAA tank closures due to the different material properties of grout versus construction concrete. Little information was found on the thermal properties of grout-type materials. Most of the literature surveyed was related to the thermal conductivity of super-plasticized grout used to seal boreholes and pipes for

<b>Mechanism</b>	<b>Causative Factors</b>	<b>Morphologic Characteristics</b>	<b>Timing of Formation</b>
Plastic shrinkage	Contraction due to water loss from surface	Large aperture, long or short	Early
Plastic settlement	Contraction due to nonuniform settlement over obstructions	Undefined	Early
Presetting	A large horizontal area of concrete makes contraction in the horizontal direction more difficult than in the vertical direction	Deep? irregular pattern	Early
Hydration shrinkage (also referred to as hygral or drying shrinkage)	Contraction due to water loss by hydration of cement	Undefined	Middle to late
Thermal stress (also referred to as thermomechanical)	Restrained expansion with heating, followed by contraction with cooling	Small aperture? long length	Middle to late
Other mechanical stresses	Extensional strain not related to water loss or temperature	Undefined	Middle to late

geothermal heat pump systems. Allan (2000) reported the coefficient of thermal expansion of the superplasticized cement–sand grout formulation designed for sealing such pipes was  $1.65 \times 10^{-5}/^{\circ}\text{C}$  [ $0.92 \times 10^{-5}/^{\circ}\text{F}$ ], approximately 60 percent greater than that of typical construction concrete and similar to neat cement. Thus, grout may be more susceptible to thermomechanical cracking than construction concrete, yet to date, no cracks within the intermediate-scale grout monolith can be conclusively linked to the thermomechanical mechanism. A maximum temperature of  $72.68^{\circ}\text{C}$  [ $163.8^{\circ}\text{F}$ ] was measured at a thermocouple located 0.3 m [1 ft] from the tank center and 0.43 m [17 in] above the bottom of the tank, approximately 23 hours after the third lift was poured (Walter, et al., 2010, Figure 3-19). The strongest temperature gradients were near the perimeter and surface of the specimen (Walter, et al, 2010, Fig. 3-19). Given this, one might expect that thermomechanical cracking, were it to occur, would happen within a ring of some width at the outer edge and surface of the monolith. However, mapped cracks on the surface of the intermediate-scale grout monolith are not consistent with a ring-shaped zone of cracks at the outer edge of the monolith.

Cracking is also influenced by the internal and external constraints on the grout; that is, by the boundary conditions provided by the structure that restrains the grout during the thermal expansion stage. Expansion cracks that form during the heating phase tend to close as the structure cools and to not be throughgoing, whereas cracks that form during the cooling phase tend to remain open and be throughgoing. The intermediate-scale grout monolith was restrained during curing by its tank liner and also by the angle-iron crossbeam used to join together the two halves of the tank. The restraint this crossbeam provided may have no direct analog to most NDAA waste tanks, and no cracks within the intermediate-scale grout monolith have been conclusively linked to expansion cracks that formed during the early curing phase.

Cracks can also be created by external stresses after the structure has cooled, such as ground settling, deformation of bounding constraints, and seismically induced stresses. Two throughgoing, linear, and narrow *en echelon* cracks that nearly bisect the monolith into two equally sized halves are interpreted as settlement cracks. Destructively removing two wall sections for analysis released restraining stresses and caused existing cracks to evolve and new cracks to form, but taking the action that led to development of these cracks has no direct analog to the NDAA case. The steel tank liner encasing the grout monolith was subject to diurnal solar heating and cooling, probably with maximum expansion/contraction occurring in the direction orthogonal to the angle-iron crossbeam, with minimum expansion/contraction occurring in the direction of the crossbeam. Buried NDAA waste tanks will not be subject to equivalent diurnal heating and cooling extremes. Much uncertainty remains regarding the degree to which external mechanical stress will affect cracking of NDAA grout monoliths.

The literature review for this report did not reveal any commercial computer codes specifically designed to simulate the complex processes influencing crack development in large concrete structures. A versatile finite element code, such as ABAQUS<sup>®</sup>, could possibly be used for this purpose because it is capable of modeling the thermomechanical behavior including time-dependent, inelastic stress–strain evolution (creep) and possibly the cracking process. Substantial effort, however, would be required to add more advanced material models to ABAQUS that would be capable of capturing the key aspects of the chemical evolution of curing grout.

Cracks were observed to continue to propagate within the intermediate-scale grout monolith during the period of this investigation. Air gap apertures between the grout mass and internal tank fixtures also evolve with curing time, as demonstrated with the initial set of 12 drum grout specimens and the sector specimen (Walter, et al., 2010). The porosity of a hydrating cement

paste decreases with time. The permeability of a newly constructed monolith decreases with porosity but increases with the development of micro- and macrocracks. Early permeability values were estimated for the intermediate-scale grout monolith in fiscal year 2010 (Walter, et al., 2010), but permeabilities that would account for parameter evolution as a function of cure time have not been reestimated since that time. Thus, staff recommend pneumatic retesting of the grout monolith. Preliminary pneumatic testing of Corehole 2, which penetrates a through-going vertical crack that nearly divides the monolith into two equal halves, indicated that the crack was highly permeable with a magnitude beyond the range of the existing pneumatic testing apparatus (Walter, et al., 2010). Staff further recommend that the permeability of this heretofore unmeasured mechanical stress crack be quantified using either pneumatic or hydraulic methods with instrumentation for high flow rates and low injection pressures.

As of the date of this report, gas injection testing of fiscal year 2010 drum grout specimens of surrogate Idaho National Laboratory (INL) heel grout and South Carolina reducing grout remains to be performed. To fulfill original project objectives, the permeabilities of 2010 drum grout specimens should be measured for two important reasons. First, the CNWRA and NRC staff received clarification on INL tank grout specifications from DOE and prepared new drum grout specimens in fiscal year 2010 that have yet to be characterized. Second, the South Carolina reducing grout specimens are a closer representation of grout that might be used to close Savannah River Site waste tanks compared to our local reducing grout specimens—several of the material components of the South Carolina reducing grout specimens are identical to those intended for NDAA use. Gas injection (i.e., permeability) tests could only have been performed on these specimens after allowing at least 30 days of curing, but no funding was available to support this work in fiscal year 2010, nor were these tests included in the fiscal year 2011 operations plan. Thus, to determine the permeability of our analog specimens for both Idaho National Laboratory heel grout and South Carolina reducing grout, staff also recommend that pneumatic testing of the fiscal year 2010 drum grout specimens be performed in fiscal year 2012.

The behavior and characteristics of the intermediate-scale grout monolith indicate that relatively large grout specimens are required to fully understand the flow behavior and cured properties of the grout that may be placed in the NDAA tanks. Further characterization of the intermediate-scale grout monolith could include

- Borescopic observations and descriptions of cracks exposed in sidewalls of Coreholes 1–9 to improve understanding of the existing three-dimensional crack systems relative to grout stratigraphy (Coreholes 3 and 5, in particular, are known to have developed cracks after core removal; furthermore, the upper half of Corehole 8 has large cracks filled with epoxy from which additional information can be gleaned that was not easily discernable from its broken overcore)
- Volumetric measurement of epoxy applied to/accepted by future coreholes as an estimate of local crack porosity
- Controlled-volume tracer experiments to characterize liquid flow and transport properties, with rapid time-lapse photography or videography used to record breakthrough times and styles
- Horizontal coring from exposed sidewalls into the center of the monolith to better capture the frequency of hydraulically important vertical cracks, which are undersampled by

vertical cores [horizontal cores would also likely reveal the thickness of the weathering rind/evaporation zone (through matrix color change) that is anticipated to surround the perimeter of the grout monolith]

- Description and color/ultraviolet photographic documentation of slabbed cores to understand the sizes of vugs, crack apertures and roughness, the composition of poorly mixed grout-ingredient inclusions, and the potential for any detrimental, long-term impacts that should be expected from such small-scale features
- Determine relationship between crack aperture and saturated permeability and relative permeability of the cracked grout; perform pneumatic testing to determine whole-monolith crack permeability with serial gas injection from multiple coreholes and packed-off intervals
- Thin section preparation and analysis to understand grout matrix porosity and color variations, microcrack porosity and connectivity, and any detrimental, long-term impacts that should be expected from clumps of poorly mixed grout-ingredient inclusions and weak aggregate particles (i.e., those which cracks penetrate through rather than traverse around)
- Characterize the mineral phases of the tan- and gray-colored matrix zones to determine the causative factors of the color variation

New grout monoliths can be constructed to

- Investigate the effect of minimized diurnal heating and cooling (as expected in an NDAA waste tank) on grout–tank wall bonds
- Investigate the effect of humidity evolution on the timing of early plastic shrinkage and later hydration and drying shrinkage crack formation (where the timing of formation is diagnostic of formation mechanism) using humidity, optical and acoustic emission sensors

If additional experimental grout monoliths are constructed under this program, staff recommend that separate pours within each lift be dyed different colors to aid identification, because some lift separations and hiatuses between pours are difficult to identify in cores.

A limited review of available literature suggests there has been substantial work performed by others who are concerned with concrete repair to understand concrete adhesion and bonding. Staff recommend a detailed review of the available literature to better place our nondestructive and destructive testing results for grout–tank wall bonding into proper context.

Staff also recommend conducting a literature review to understand whether there may be detrimental, long-term impacts from incomplete mixing of grout material components. CNWRA staff do not currently have enough information to indicate whether thermal cracking of grout should be expected in an actual NDAA tank. CNWRA staff recommend NRC consider a scope of work that includes measuring (i) the evolution of grout thermal conductivity and the (ii) heat generation rate of grout, and numerical modeling and model calibration of the intermediate-scale grout monolith to achieve the previously measured temperature distribution (Walter, et al., 2010, Fig. 3-19), followed by upscaling the model to an NDAA-tank scale to

ascertain whether sufficient thermal-cracking-magnitude temperature gradients could be realized in an NDAA tank.

Finally, degradation characteristics and leach resistance of engineered analogs from the low-level waste and transuranic (intermediate-level) waste programs of various nations might be examined under this program in the future, with the caveat that emplacement mechanisms differ in significant ways, and thus material and chemical properties may also differ to significant degrees.

## REFERENCES

Allan, M.L. "Materials Characterization of Superplasticized Cement-Sand Grout." *Cement and Concrete Research*. Vol. 30, No. 6. pp. 937–942. 2000.

Springenschmid, R., ed. "Preface." *Thermal Cracking in Concrete at Early Ages*. Spon, London: E&FN. 1994.

Walter, G.R., C.L. Dinwiddie, D. Bannon, G. Frels, and G. Bird. "Intermediate Scale Grout Monolith and Additional Mesoscale Grout Monolith Experiments: Results and Recommendations." Status Report. San Antonio, Texas: Center for Nuclear Waste Regulatory Analyses. September 2010.

Walter, G.R., C.L. Dinwiddie, E.J. Beverly, D. Bannon, D. Waiting, and G. Bird. "Mesoscale Grout Monolith Experiments: Results and Recommendations." San Antonio, Texas: Center for Nuclear Waste Regulatory Analyses. July 2009.

## ACKNOWLEDGMENTS

This report was prepared to document work performed by the Center for Nuclear Waste Regulatory Analyses (CNWRA<sup>®</sup>) for the U.S. Nuclear Regulatory Commission (NRC) under Contract No. NRC-02-07-006. The activities reported here were performed on behalf of the NRC Office of Federal and State Materials and Environmental Management Programs, Division of Waste Management and Environmental Protection. This report is an independent product of CNWRA and does not necessarily reflect the view or regulatory position of NRC.

The authors wish to thank F. Hawkins for his quality assurance oversight and audit, L. Mulverhill for her editorial review, S. Stothoff for his technical review, E. Percy for his programmatic review, and L. Selvey for her secretarial support. The authors also thank Coeur Products for providing core boxes for core samples at no cost.

## QUALITY OF DATA, ANALYSES, AND CODE DEVELOPMENT DATA

**DATA:** All CNWRA-generated data contained in this report meet quality assurance requirements described in the Geosciences and Engineering Division Quality Assurance Manual. Sources of other data should be consulted for determining the level of quality of those data. The work presented in this report is documented in Scientific Notebooks 1033 (Walter, et al., 2011) and 1074 (Light, et al., 2011).

**ANALYSES AND CODES:** No CNWRA-developed codes were used to analyze data for this report. The following commercial off-the-shelf software packages were used for analysis: ESRI ArcGIS<sup>®</sup> Version 9.2. Figures were produced using Adobe<sup>®</sup> Photoshop<sup>®</sup> Version CS5 (Adobe Systems, Inc., 2010a) and Adobe<sup>®</sup> Illustrator Version CS5 (Adobe Systems, Inc, 2010b). All commercial off-the-shelf software packages used in this report are under Technical Operating Procedure 18 control.

## REFERENCES

Adobe Systems, Inc. "Adobe<sup>®</sup> Photoshop<sup>®</sup>." San Jose, California: Adobe Systems, Inc. 2010a.

Adobe Systems, Inc. "Adobe Creative Suite—Adobe Illustrator<sup>®</sup>." San Jose, California: Adobe Systems, Inc. 2010b.

ESRI, Inc. "ArcGIS Version 9.2." Redlands, California. 2006

Light, G., S. Winterberg, and C.L. Dinwiddie. "NDE Evaluation of Bonding to Large Grout Tank." Scientific Notebook 1074 & CD. San Antonio, Texas: CNWRA. pp. 1-33. 2011.

Walter, G.R., C.L. Dinwiddie, and D.J. Waiting. "2010 Small-Scale Grout & Grout Coring." Scientific Notebook 1033. San Antonio, Texas: CNWRA. pp. 1-80. 2011.

# 1 BACKGROUND AND SCOPE OF REPORT

Under Section 3116 of the Ronald W. Reagan National Defense Authorization Act of Fiscal Year 2005 (NDAA), the U.S. Nuclear Regulatory Commission (NRC) is responsible for consulting with the U.S. Department of Energy (DOE) on the DOE waste determinations for certain waste tanks and vaults at the Savannah River Site (SRS) and Idaho National Laboratory (INL), and for monitoring disposal actions taken by DOE pursuant to NDAA Section 3116, Subsection (a)(3), Subparagraphs (A) and (B) for the purpose of assessing compliance with the performance objectives of 10 CFR Part 61, Subpart C. The NDAA provides criteria to determine whether certain waste resulting from the reprocessing of spent nuclear fuel is not high-level waste and specifies that the performance objectives in 10 CFR Part 61, Subpart C must be met.

Under the provisions of this Act, DOE may stabilize waste tanks and vaults with cementitious materials, such as grout. Cementitious materials may be formulated to produce waste forms that enhance waste isolation by limiting radionuclide release and migration. DOE may rely on (i.e., take credit for) natural and engineered system properties that provide attenuation and retardation of radionuclide migration as part of its waste disposal system performance assessments. NRC staff use information from independent analyses to support their consultation responsibilities for non-high-level, waste-incident-to-reprocessing determinations and their monitoring responsibilities for subsequent actions taken under the NDAA. To this end, the Center for Nuclear Waste Regulatory Analyses (CNWRA<sup>®</sup>) has been tasked to provide mechanistic information on the physical and chemical degradation of cementitious waste forms that are used for the isolation and containment of radioactive wastes and to evaluate the potential for radionuclide bypass of the engineered barriers via preferential or fast pathways.

Previous reviews of DOE waste determinations indicated that potential fast pathways going through and bypassing barriers may dominate waste release from large, grout-filled tanks and vaults. Thus, macrocrack density and connectivity may play major roles in the release of radionuclides from *in-situ* tank closures and monolithic waste forms, such as saltstone. Review of experimental and observational data on mass transport properties of cementitious materials did not reveal empirical data from which to estimate the likely properties of macrocracks that may develop in large grout monoliths. Most crack characterization measurements to date have been made on small-scale laboratory specimens using construction materials with significantly different formulations than those DOE proposed for radioactive waste disposal at NDAA facilities. Additionally, no data are available to assess the significance of annular gaps that may develop between cementitious grout and internal tank fixtures (e.g., interior tank walls, pipes, and cooling coils). Lack of relevant data represents a key uncertainty when evaluating DOE waste determinations that rely on cementitious grout integrity to meet the performance objectives for low-level waste found in 10 CFR Part 61, Subpart C.

To establish a base-level understanding of the potential for fast flow cracks and annular gaps to form soon after grout is emplaced in a waste tank, CNWRA staff developed mesoscale grout monolith specimens in fiscal year 2009 at Southwest Research Institute<sup>®</sup> (SwRI<sup>®</sup>) facilities in San Antonio, Texas, as analogs to grouted tanks at NDAA facilities (Walter, et al., 2009, 2010). Mesoscale specimens were constructed in 55-gallon drums and also in a 3 m [10 ft] by 30° arc sector to help inform development of conceptual designs for larger-scale grout monolith experiments. The mesoscale grout monolith specimens, which were constructed using grout formulations similar to those being considered for use at the SRS and INL, were instrumented to permit (i) observation and quantification of the effects of macrocracks, annuli between grout and internal fixtures or container walls, and lift separations that may develop due to thermal

contraction cracking, shrinkage, and the passage of time between lift emplacements, and (ii) the conduct of gas permeability tests.

These experiments led to the design, development, and preliminary testing of an intermediate-scale grout monolith cylindrical specimen in fiscal year 2010, which was 6.1-m [20-ft] diameter and approximately 0.8 m [30 in] high composed of Local Reducing Grout (Walter, et al., 2010). The scale of this specimen is approximately one-fourth that of typical NDAA tanks. The grout was mixed at a batch plant operated by Lattimore Materials Company using the nominal formulation listed in Table 1-1. This formulation was based on a formulation reported for Alternative Reducing Grout in Langton and Cook (2008) and Langton, et al. (2007). However, the reducing grout used in the intermediate-scale grout monolith was not identical to grout tested by Langton, et al. (2007) because the sources of the Portland cement, sand, and fly ash were different. In addition, the quantity of water and high range water reducer (Sika Viscocrete, 2100) used in the grout batch for the intermediate-scale grout monolith were adjusted to achieve a self-leveling grout with zero bleed and, thus, were not the same as used by Langton, et al. (2007).

The grout was transported from the batch plant to the test site in cement mixing trucks. Nominal batch volumes varied from 3.9 to 4.6 m<sup>3</sup> [5 to 6 cubic yards] per truck. The actual grout formulations and batch volumes are listed in Table 1-1. The actual yield volumes were approximately 90 percent of the nominal volumes. Grout was transferred from the delivery trucks to the intermediate scale grout monolith tank using a boom pump truck. The discharge line of the pump truck was positioned near the center of the tank.

During the current fiscal year, testing and analysis of the intermediate-scale grout monolith specimen continued, including (i) nondestructive and destructive testing of bonds between grout and tank walls; (ii) additional core sampling, inspection, and description; and (iii) surface crack characterization. This letter report fulfills the requirement for CNWRA to document the results of these continuing analyses and also documents a literature review on the topic of mechanisms affecting crack formation in massive concrete structures. We conclude with recommendations for future work in fiscal year 2012.

The intent of CNWRA grout monolith investigations is to gain insight into risk-significant aspects of grout behavior and properties that affect performance. Due to differences in the formulations of the grouts used in these investigations and differences in the conditions of placement and the environmental conditions of curing, the findings reported here may not represent the behavior and properties of grouts used in actual closure of NDAA tanks. We are unaware of equivalent studies performed with the material components of NDAA tank grouts, nor have we received final recipes for grouts intended to be used for tank closure at the Savannah River Site, South Carolina. Because the U.S. Department of Energy has not supplied grout monolith performance information of an equivalent nature, NRC staff will likely use the independently acquired information contained within this and predecessor reports to support their consultation responsibilities for non-high-level, waste-incident-to-reprocessing determinations and their monitoring responsibilities for subsequent actions taken under the NDAA.

Table 1-1. Summary of Grout Batch Quantities, Flow Measurements, and Weather Conditions During Pours								
Material	Nominal Quantity	Actual Quantities Per Cubic Yard*						
		Batch 1 02 Mar 2010	Batch 2 02 Mar 2010	Batch 3 03 Mar 2010	Batch 4 03 Mar 2010	Batch 5 04 Mar 2010	Batch 6 04 Mar 2010	Batch 7 04 Mar 2010
Portland Cement Type I/II (lbm)†	303	300	302	304	280	304	301	298
River Sand (lbm)	1414	1420	1420	1423	1500	1420	1420	1420
Slag Cement (lbm)	303	310	306	302	303	304	306	318
Fly Ash (lbm)	790	788	787	788	787	786	791	816
Water (lbm)	Up to 524	428	414	409	408	417	421	467†
RECOVER Hydration Stabilizer (oz)‡	Up to 10	5	5	5	5	5	5	5
Sika Viscocrete 2100 (oz)	Up to 50	30§	30	30	30	35	34	35
Kelco-crete DG (gm)	217	216	216	216	216	216	216	216
Nominal Batch Volume (yd <sup>3</sup> )		6	6	6	6	5	5	5
Puddle Spread (in)¶	30	26	29.5	28	26.5	24.5	29	31.5#
Bleed (wt%)	0	0	0	<1	0	0	0	0
w/c#	Up to 0.38	0.31	0.30	0.29	0.30	0.30	0.30	0.33
Delivery Time (minutes)**		55	32	30	21	30	35	30

Table 1-1. Summary of Grout Batch Quantities, Flow Measurements, and Weather Conditions During Pours (continued)								
Material	Nominal Quantity	Actual Quantities Per Cubic Yard*						
		Batch 1 02 Mar 2010	Batch 2 02 Mar 2010	Batch 3 03 Mar 2010	Batch 4 0 3Mar 2010	Batch 5 04 Mar 2010	Batch 6 04 Mar 2010	Batch 7 04 Mar 2010
Weather Conditions at 1455††								
Sky		Clear		Clear		Clear		
Temperature (°C)		15.6		19.4		20.5		
Relative Humidity (%)		38		37		45		
Wind Speed (kph)		13		6		22		
*1 yd <sup>3</sup> = 0.77 m <sup>3</sup> †1 lbm = 0.45 kg ‡1 oz = 29.6 ml §Sika Viscocrete increased to 30 oz [870 ml] after slump spread test at batch plant; increase is not recorded in the batch record from Lattimore Materials   Actual yield approximately 90 percent of nominal volume ¶Average diameter per ASTM C 1611 (ASTM International. "Standard Test Method for Slump Flow of Self-Consolidating Concrete." C 1611/C 1611M-09b. West Conshohocken, Pennsylvania: ASTM International. 2009.); 1 in = 2.54 cm #Added 250 lbm [30 gal] water at site, mixed 10 minutes **Time from leaving batch plant to arriving at site ††Weather conditions at KellyUSA Airport from < <a href="http://www.wunderground.com/history/airport/KSKF/2010/3/2/DailyHistory.html?req_city=NA&amp;req_state=NA&amp;req_statenname=NA">http://www.wunderground.com/history/airport/KSKF/2010/3/2/DailyHistory.html?req_city=NA&amp;req_state=NA&amp;req_statenname=NA</a> > (09 March 2010)								

## 2 TESTING OF BOND BETWEEN GROUT AND TANK WALL

CNWRA conducted tests to determine the quality of the bond that may develop between tank-waste-stabilizing grout and tank walls or liners. It is important for the stabilizing grout to bond to the waste tank liner to minimize the potential for thin water films or rivulets to enter a gap between the grout mass and tank wall liner. The concern is that water films or rivulets could rapidly flow through such gaps down into the residual contamination zone at the base of the tank. Much of the waste remaining in NDAA tanks will be on tank surfaces.

To determine whether grout in the intermediate-scale grout monolith was well bonded to the tank liner at various locations, SwRI Mechanical Engineering Division developed a field ultrasonic inspection technique applied to the outside wall of the tank to evaluate the occurrence of grout delaminations from the tank wall (i.e., air gaps between the grout and tank wall). The principle of the technique is discussed in Section 2.1, and the ultrasonic data collected and results obtained are discussed in Section 2.2. Destructive testing, discussed in Section 2.3, was conducted by removing two tank wall sections to correlate the ultrasonic results with the actual condition of the grout mass surfaces and the grout residue remaining on the inside surface of the tank wall. Dynamic structured light (DSL) imaging of the grout residue interior to each wall section, discussed in Section 2.4, was undertaken to produce surface roughness maps of the actual condition on the inside surface of the tank walls.

### 2.1 Conceptual Solution Using Ultrasonic Inspection

#### 2.1.1 Theory

SwRI Mechanical Engineering Division developed a method (Light, et al., 2011) to estimate the likelihood of an air gap inside the tank wall using measurements on the outer tank wall. The method uses ultrasonic energy applied to the outer side of the tank wall and propagates it into the tank wall. It is assumed that some of the ultrasound would propagate into the grout if grout was bonded to the tank wall; but ultrasound would resonate only in the tank wall if there was an air gap between the grout and tank wall.

The concept is illustrated in Figure 2-1. Again, the assumption is that there will be an air gap where the grout has not bonded to or has debonded from the tank wall. The ultrasonic reflection coefficient,  $R_p$ , is given by

$$R_p = \text{Reflection}_{\text{pressure}} = (Z_2 - Z_1)/(Z_2 + Z_1) = \Delta Z/\Sigma Z \quad (2-1)$$

where  $Z_2$  is the acoustic impedance of the second material (air or grout in this case) and  $Z_1$  is the acoustic impedance of the first material (steel in this case). The transmission into the second material,  $T_p$ , is given by

$$T_p = \text{Transmission}_{\text{pressure}} = 1 - R_p \quad (2-2)$$

If there is an air gap behind the steel tank wall, then the ultrasonic pressure ( $R_p + T_p$ ) will be nearly 100 percent reflected at the steel–air interface and will reverberate in the tank wall with essentially no transmission into the grout (Figure 2-1). If there is no air gap, then approximately 30 percent of the ultrasonic pressure will be transmitted into the grout and 70 percent will be reflected at the interface (Figure 2-1). This represents a 3 decibel shift.

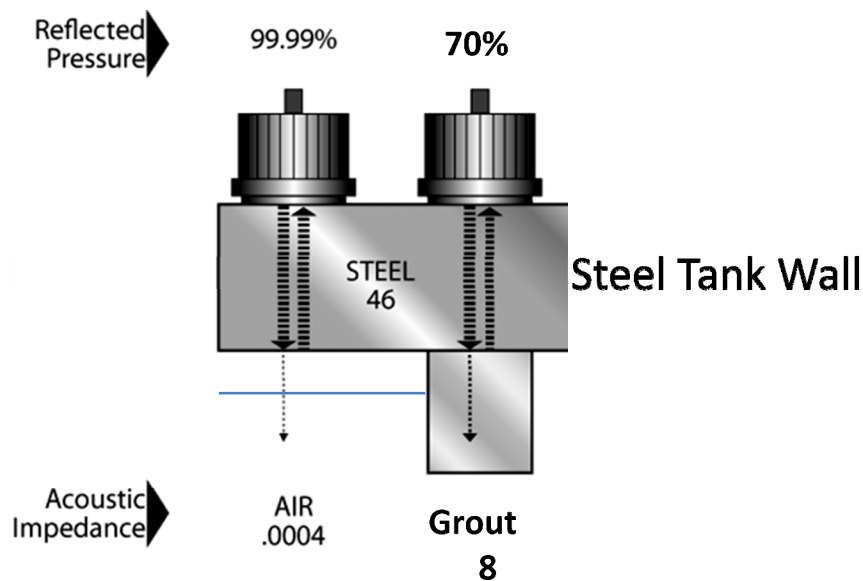


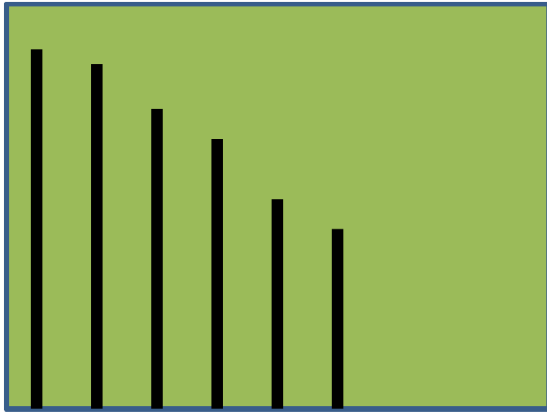
**Figure 2-1. Illustration of the Reflection of Ultrasonic Waves From a Steel–Air and Steel–Grout Interface**

If a pulse echo ultrasonic technique is used, it is anticipated that where there is an air gap between the grout and tank wall, the ultrasonic signal would reverberate many times in the steel wall, which has low ultrasonic attenuation. For the case where there is no air gap, the energy would quickly dissipate into the grout. Schematically, this is illustrated in Figure 2-2.

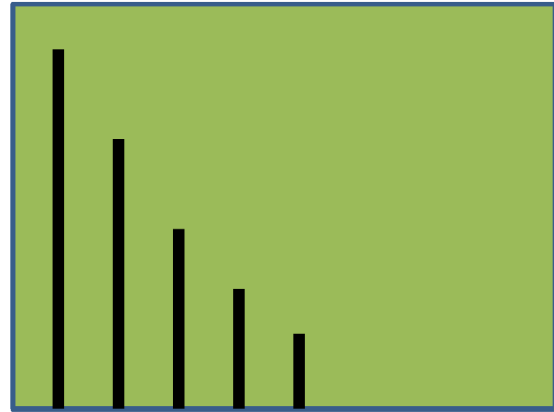
### **2.1.2 Laboratory Tests and Data Collected From Mesoscale Drum Grout Specimens**

A small test sample of grout in a steel and wooden form, which was designed and built to verify the ultrasonic inspection theory, served instead to suggest poor grout bonding behavior. The bottom of the form was a 6.35-mm [ $\frac{1}{4}$ -in]-thick steel plate (similar to the tank wall) with porous cardboard cutouts, representing air gaps, secured to the steel plate. The sides of the form were wooden 2 × 4s. Local Reducing Grout (Walter, et al., 2010) was mixed and poured into the form. After approximately 3 days of curing, the form was gently turned on its side to enable access to the steel plate, but the grout immediately fell out of the form. Clearly, the grout was not bonded to either the steel plate with cardboard cutouts or to the wooden sides of the form. At this point, staff turned their attention to verifying the theory using existing mesoscale drum grout specimens for which there were observations of grout that had pulled away from the drum wall, at least at the surface (Walter, et al., 2009).

Ultrasonic test results were obtained from several of the drum grout specimens within the upper, middle, and lower lifts. Results are presented as the number of multiple reflections above the midscreen level of the oscilloscope (Figures 2-3). Examples of ultrasonic data collected are shown in Figure 2-4 for inferred no-air-gap (Tank T7 middle lift) and air-gap (T6 upper lift) cases. These data look very similar to illustrations shown in Figure 2-2.



**UT Signal Amplitude with an Air Gap**



**UT Signal Amplitude without an Air Gap**

**Figure 2-2. Illustration of the Expected Ultrasonic Signal Amplitude Data Obtained From a Pulse-Echo Transducer Placed on the Steel Wall With a Steel–Air Interface (Left) and a Steel–Grout Interface (Right)**

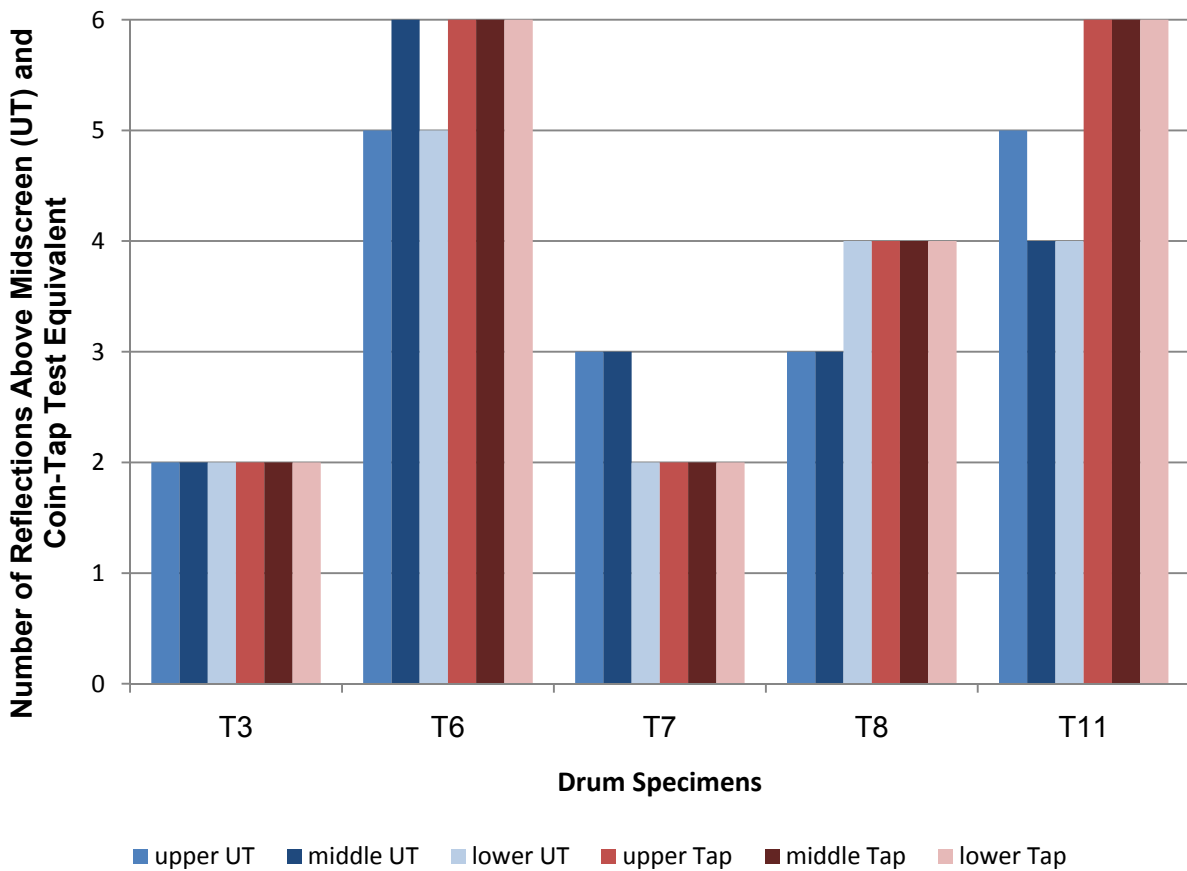


**Figure 2-3. Ultrasonic and Coin-Tap Test Results for Each Lift Within Five Drum Grout Specimens. High Values Suggest Air Gaps and Low Values Suggest the Absence of Air Gaps.**

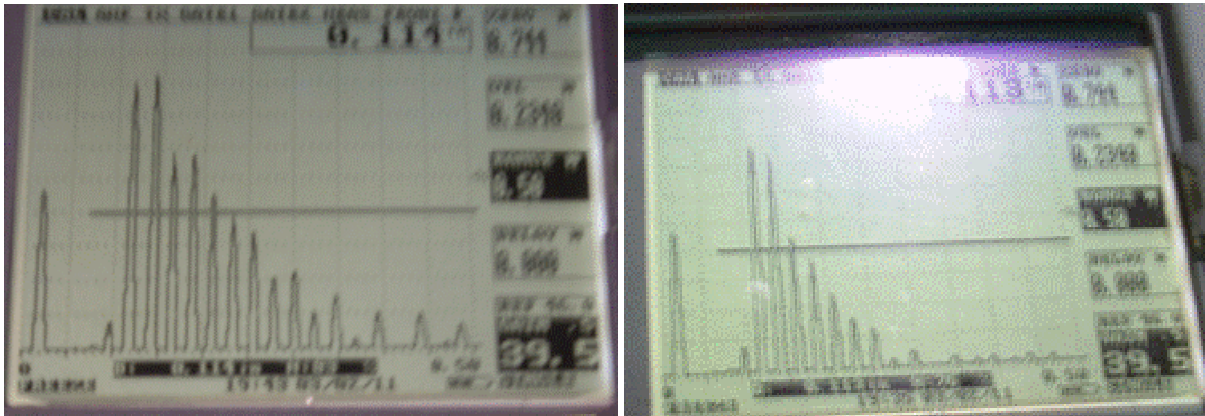


**Figure 2-4. Ultrasonic Signal Amplitude Data Collected From Drum Grout Specimens With an Air Gap (Left) and Without (Right) an Air Gap (Compare With Schematic Illustration of Figure 2-2)**

As an additional analysis, coin-tap test (e.g., Hsum, et al., 2009) data (Figure 2-3) were also collected from the drum grout specimens. The tap test was conducted by tapping a quarter (25¢ coin) on the outside surface of the drum, which yielded a damped thudding sound for the no-air-gap case and a hollow, higher pitched sound for the air-gap case. This is a very qualitative measurement and depends heavily upon the inspector conducting the tap test. The tap test is most often used to detect large debonds. Given the qualitative nature of tap test results, numerical categories were selected to indicate the range of audible frequencies that were heard by the inspector (i.e., low frequency was assigned the value 2, intermediate frequency was assigned the value 4, and the higher frequency sound was assigned the value 6.) The lower frequency corresponded to a no-air-gap region, while the highest frequency corresponded to an air-gap region.

In this application, it is thought that the coin-tap test could detect cases where the grout had a significant air gap between the grout–tank wall and the grout. This condition might be representative of large regions of honeycombing. The ultrasonic results, meant to verify theory and enable a go/no-go decision for use of the ultrasonic method at the intermediate-scale grout monolith, agreed well with the coin-tap test and were sufficiently encouraging that staff proceeded with ultrasonic testing of the intermediate-scale grout monolith.

## **2.2 Ultrasonic and Coin-Tap Test Data Acquisition From Intermediate-Scale Grout Monolith and Results**

The intermediate-scale grout monolith tank is described by Walter, et al., (2010). The tank has a circumference of 19 m [62.8 ft] and its wall is composed of 0.63-cm [ $\frac{1}{4}$ -in]-thick carbon steel. Thirty-six percent of the tank wall was investigated using ultrasonic testing. The tank wall was gridded into four 173-cm [68-in]-long sections, each having a 5-cm  $\times$  5-cm [2-in  $\times$  2-in] grid pattern (Figures 2-5 through 2-8). Ultrasonic pulse-echo data were collected using a Panametrics V126, 5 MHz, 0.95-cm [0.375 in]-diameter transducer. Results are shown in Figures 2-5 through 2-8. In addition to the ultrasonic tests, coin-tap tests were also performed to provide a qualitative indication of bonding. The coin-tap test was performed within each grid

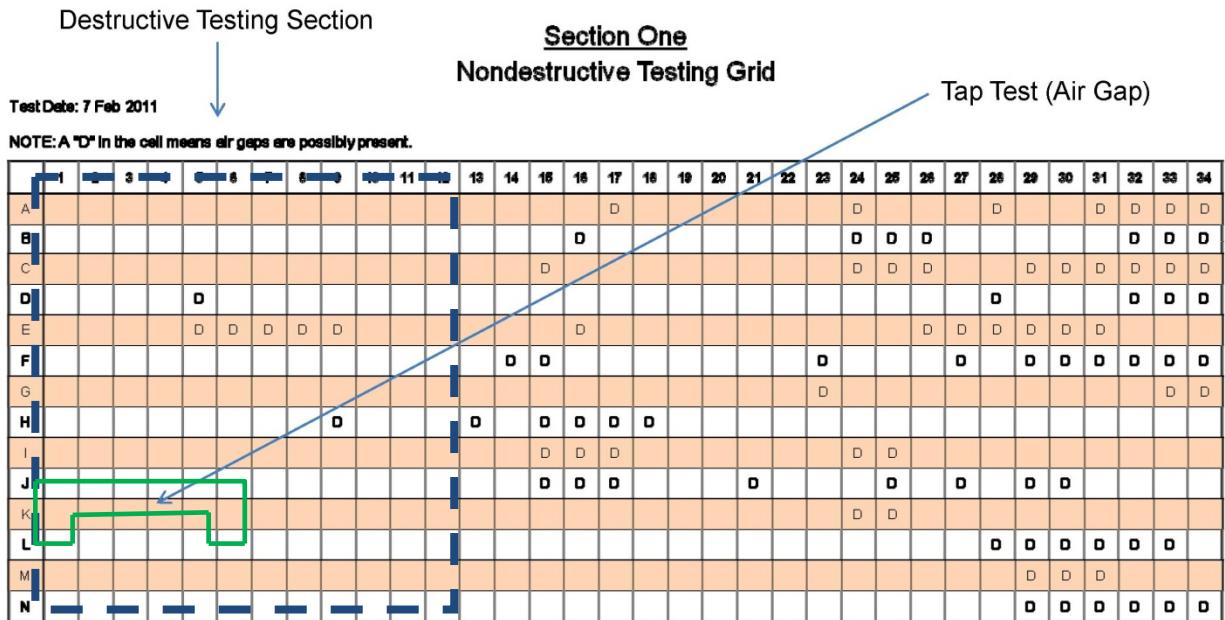


**Figure 2-5. Illustration of the Section One Grid on the Tank Wall Shows Cells Where an Air Gap Was Detected (D) Between the Tank Wall and the Grout Using Ultrasound, Regions Where the Coin-Tap Test Indicated Possible Air Gaps, and a Representative Region Free From Air Gaps That Could Be Destructively Removed for Additional Analysis. Grid Cells Are 5 × 5 cm<sup>2</sup> [2 × 2 in<sup>2</sup>]**

cell, as described previously for the drum specimens, and results are presented in Figures 2-5 through 2-8.

### 2.3 Destructive Testing Results

On 1 April 2011, two sections of the tank wall, each approximately 0.6-m [24-in]-wide by tank height (see Figures 2-5 and 2-7) were cut from the tank using a rotary saw. The ultrasonic data suggest the wall section shown in Figure 2-5 had few air gaps, and thus it was inferred to be well-bonded to the grout mass. When this section was cut out, it had to be pried free from the grout monolith, and the effort to accomplish this took 5–10 minutes. The ultrasonic data suggested the section shown in Figure 2-7 had many air gaps, and thus it was inferred to be poorly bonded to the grout mass. When this tank wall section was cut out, it was easily pulled away from the grout mass, consistent with the state of being poorly bonded. Grout adjacent to these tank wall sections is shown in Figures 2-9 and 2-10. The air-gap-free section has a relatively smooth surface, especially in the two lower lifts. The section that had air gaps has a relatively rough surface, especially in the upper two lifts. Smoother grout may correspond to more favorable permeabilities: the results of gas injection testing (Walter, et al., 2010) indicated a decrease in permeability with depth.

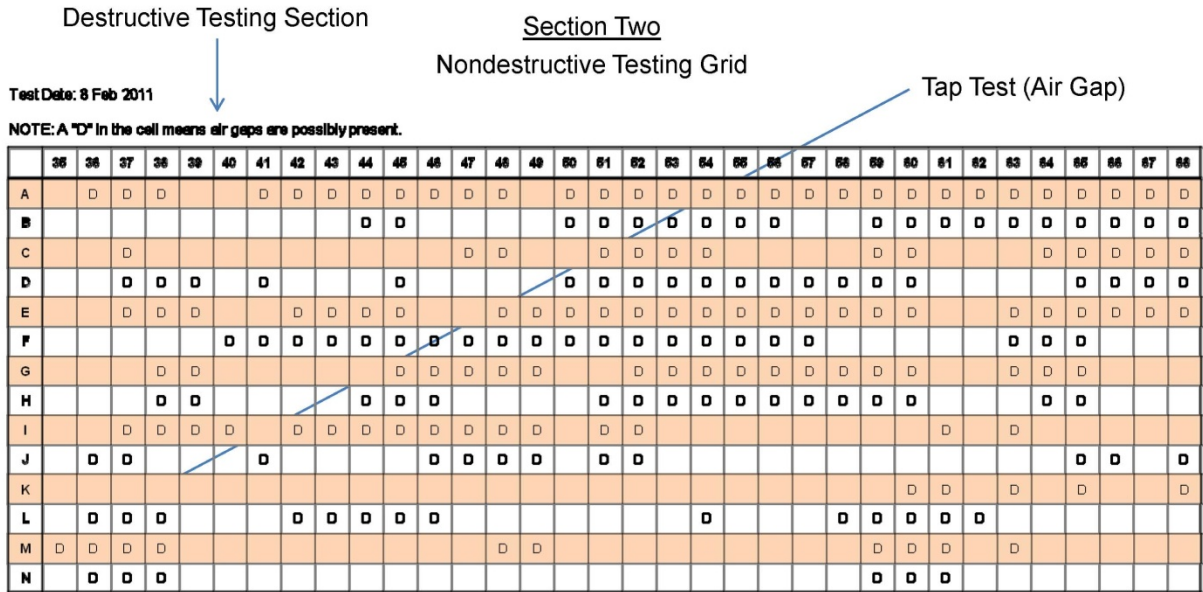


Figure 2-6. Illustration of the Section Two Grid on the Tank Wall Shows Cells Where an Air Gap Was Detected (D) Between the Tank Wall and the Grout Using Ultrasound

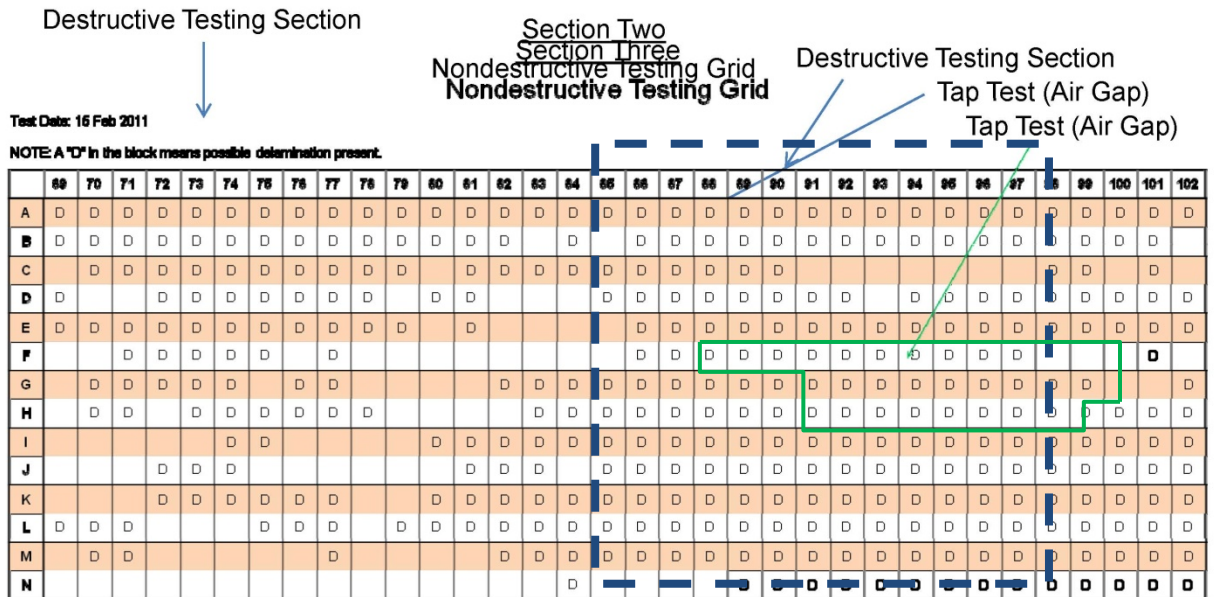


Figure 2-7. Illustration of the Section Three Grid on the Tank Wall Shows Regions Where an Air Gap Was Detected (D) Between the Tank Wall and the Grout Using Ultrasound, Regions Where the Coin-Tap Test Indicated Possible Air Gaps, and a Representative Region of Air Gaps That Could Be Destructively Removed for Additional Analysis

**Section Four  
Nondestructive Testing Grid**

Test Date: 24 Mar 2011

NOTE: A "D" in the cell means an air gap is possibly present

	103	104	105	106	107	108	109	110	111	112	113	114	115	116	117	118	119	120	121	122	123	124	125	126	127	128	129	130	131	132	133	134	135	136		
A	D	D	D	D	D		D	D	D	D	D	D	D	D	D			D	D			D	D						D		D		D	D		
B	D	D	D	D				D	D	D	D	D	D	D	D	D	D	D	D					D					D	D		D	D		D	
C	D	D	D	D	D			D	D	D	D	D	D	D	D	D			D				D	D	D			D	D	D			D	D		
D	D		D	D	D			D	D	D	D	D	D	D			D	D	D			D		D	D	D			D				D	D		
E	D							D	D	D	D	D	D	D	D	D	D	D	D	D	D	D	D	D	D	D			D	D	D	D	D	D		
F		D	D	D				D	D	D		D	D	D	D	D	D	D					D	D			D	D	D	D	D	D	D		D	
G	D	D	D						D		D	D	D	D	D	D	D	D	D	D	D	D	D	D	D	D			D	D	D	D	D	D	D	
H	D	D	D	D	D			D	D	D	D	D	D	D	D	D			D	D	D	D	D					D		D	D					
I	D	D	D	D				D	D	D	D	D	D	D	D	D	D	D	D	D	D	D	D					D		D	D	D	D	D	D	D
J	D	D		D				D	D	D	D	D	D	D	D	D	D	D	D	D	D	D	D					D		D	D	D	D	D	D	D
K	D	D	D	D	D			D	D	D	D	D	D	D	D	D	D	D	D	D	D	D					D	D		D	D	D	D	D	D	D
L	D	D	D	D	D			D	D	D	D	D	D	D	D	D	D	D	D			D						D	D	D		D		D	D	
M	D	D	D	D				D	D	D	D	D	D	D	D	D			D									D	D	D	D	D	D	D	D	
N	D	D		D	D			D				D					D													D	D			D	D	

**Figure 2-8. Illustration of the Section Four Grid on the Tank Wall Shows Regions Where an Air Gap Was Detected (D) Between the Tank Wall and the Grout Using Ultrasound**

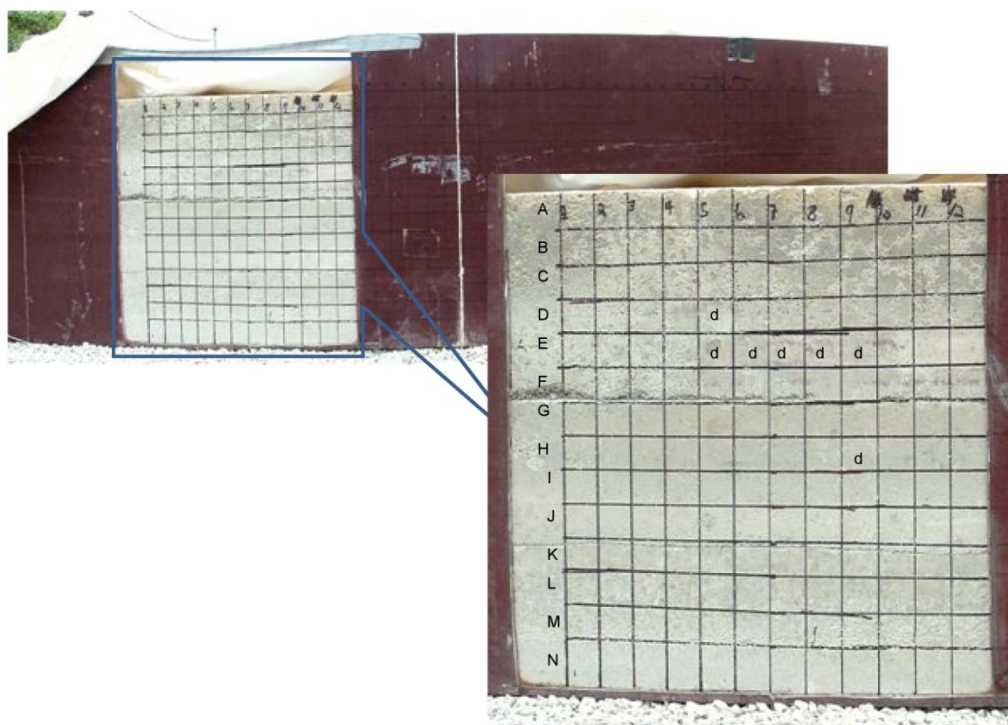


**Figure 2-9. Photographs of the Grout Surface Adjacent to the Removed Tank Wall Within the Section One Grid (cf. Figure 2-5)**

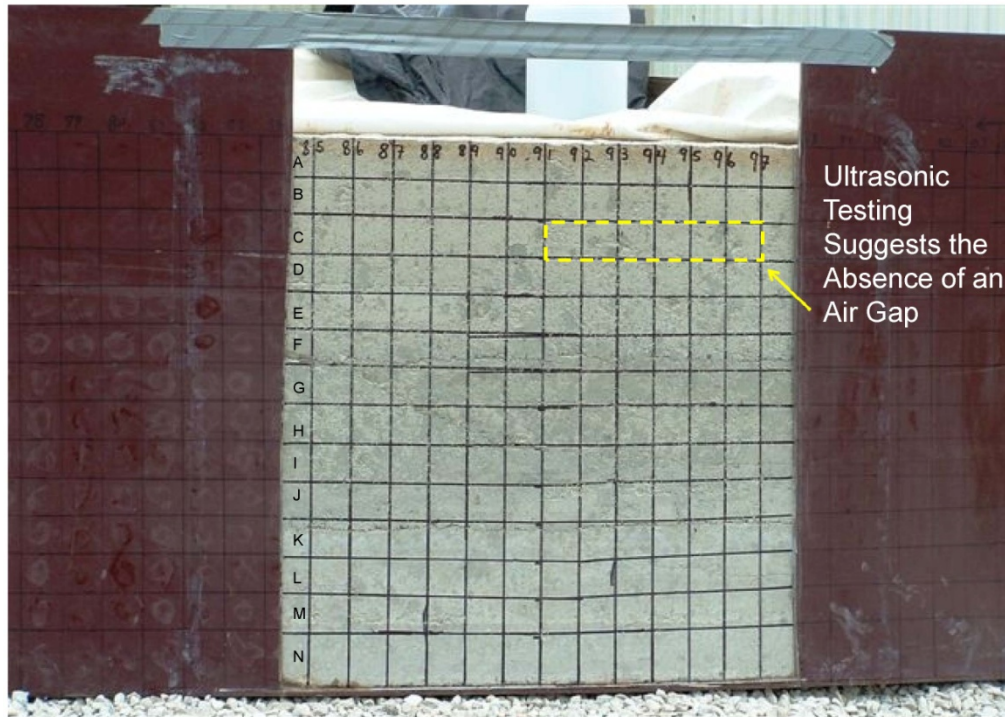


**Figure 2-10. Photograph of the Grout Surface Adjacent to the Removed Tank Wall Within the Section Three Grid (cf. Figure 2-7)**

Photographs of Section One grout regions C5–F9 (Figure 2-11) and G5–J9 (Figure 2-12) show that much of the surface is smooth, indicating very close, if not intimate, contact with the tank wall. Photographs of Section Three grout regions C89–F92 (Figure 2-13), G90–J95 (Figure 2-14), A92–D98 (Figure 2-15), and J85–N90 (Figure 2-16) illustrate variations in surface condition ranging from smooth to rough.

## **2.4 Surface Morphology of Excised Tank Wall Sections Using Dynamic Structured Light**

### **2.4.1 Method**

SwRI staff used DSL to examine the interior surface roughness of sections removed from the intermediate-scale grout monolith steel retaining wall. The DSL device, developed at SwRI, uses the moving shadow edge of patterned incident light to create a very high resolution digital elevation model (DEM) (Franke, et al., 2003). Here, horizontal resolution is approximately 0.273 mm/pixel [0.011 in/pixel], and vertical resolution is approximately 0.0127 mm [0.0005 in]. As configured for this application, a single DSL DEM image covers an 18-cm [6.1-in]-tall arcuate swath contained within a 27.94-cm [11-in] square footprint. Each DSL footprint is photographed using a digital camera. The DEMs and photographs are uniformly scaled, coregistered, and transformed to a rectangular coordinate system to maintain spatial fidelity.

Within even a single DSL image, the curvature of the tank wall is much greater than the relief related to surface roughness, with the result that contouring of the data is dominated by the relief related to curvature of the tank wall. However, surface roughness was easily observed and well represented using digital shaded relief (DSR) models constructed using

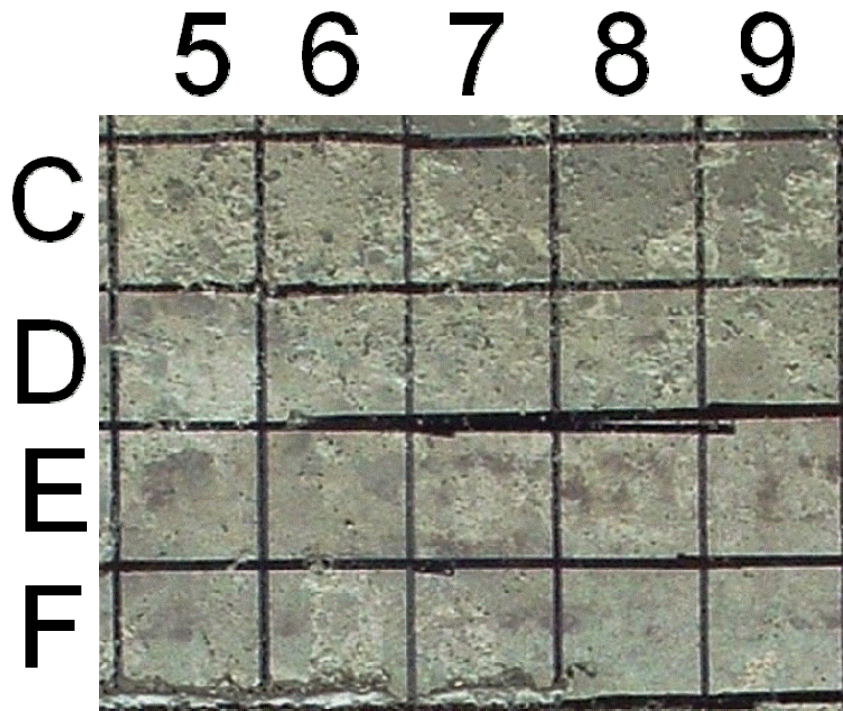


**Figure 2-11. Photograph of Section One Grout Near the Base of Lift 3, Which Was Predicted by Ultrasonics To Be Free From Air Gaps. Much of the Lift 3 Surface in the Lower Half of the Photo Is Smooth. Near the Top, There Is More Pitting. Evidence of Preexisting Grout Splatters From Prior Pours Is Observed.**

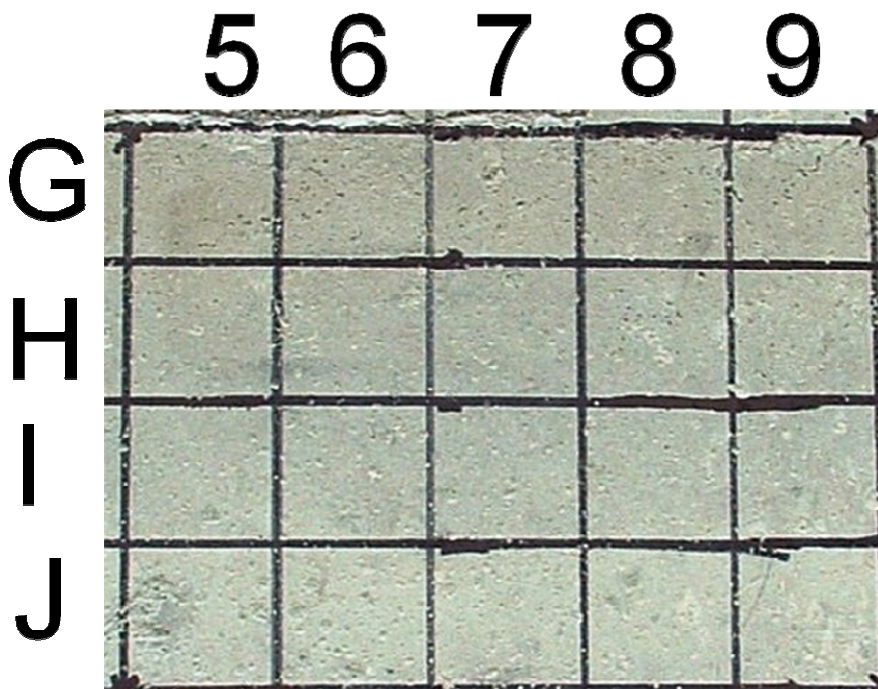


**Figure 2-12. Photograph of Section One Grout at the Top of Lift 2, Which Was Predicted by Ultrasonics To Be Free From Air Gaps. Most of the Lift 2 Surface Is Smooth. Few Grout Splatters Are Observed.**

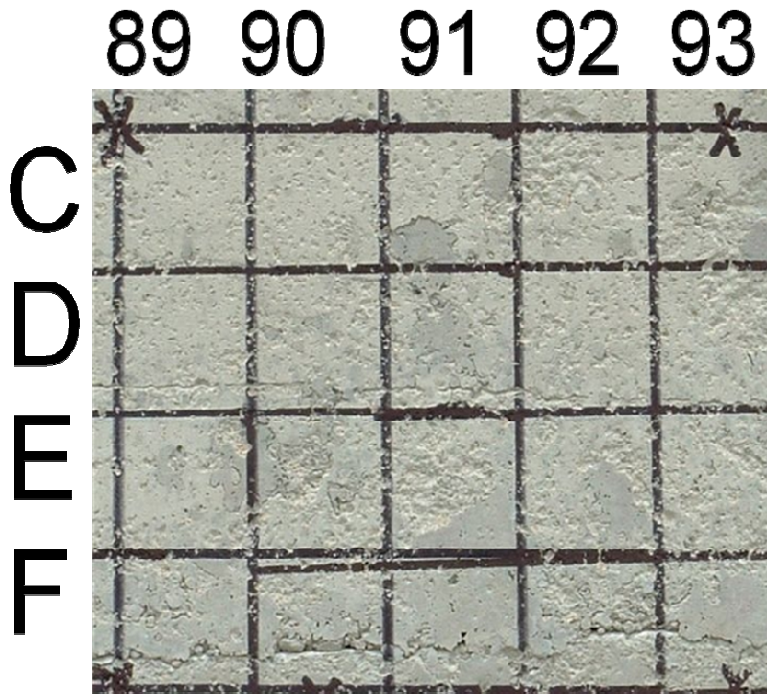


Figure 2-13. Photograph of Section Three Grout, Which Was Predicted by Ultrasonics To Have Air Gaps. Much of the Surface Is Pitted and Rough. Evidence of Preexisting Grout Spatters From Prior Pours Is Observed.

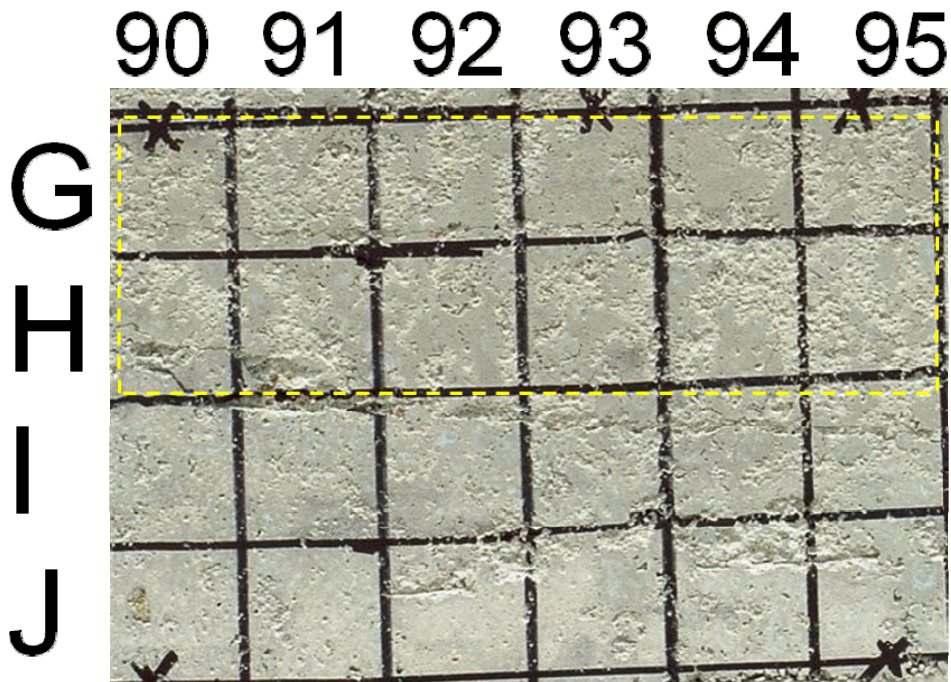


Figure 2-14. Photograph of Section Three Grout, Which Was Predicted by Ultrasonics To Have Air Gaps. Most of the Surface Is Pitted and Rough and Cracks Are Present. The Dashed Outline Encloses an Area Where the Coin-Tap Test Indicated Air Gaps Were Present.

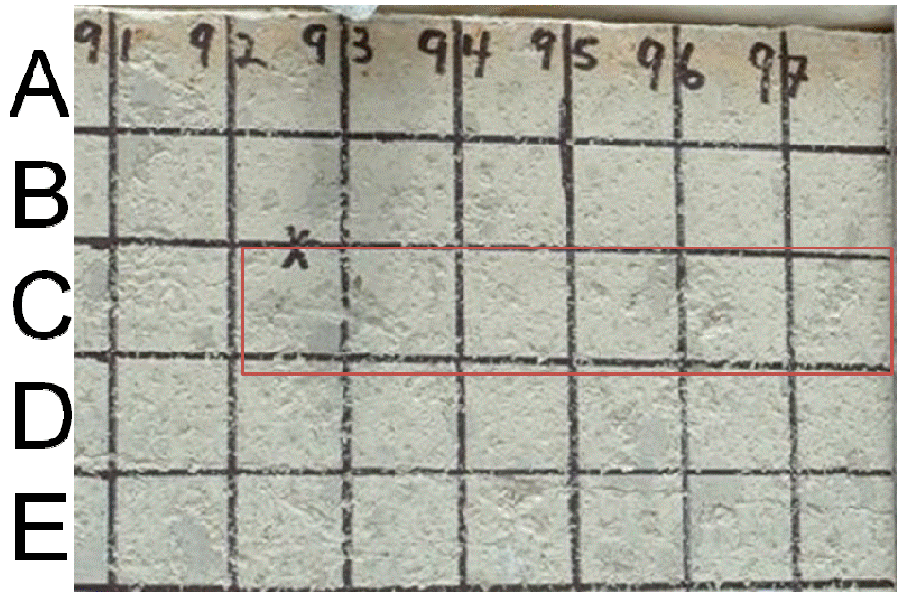


Figure 2-15. Photograph of Section Three Grout, Which Was Predicted by Ultrasonics To Have Air-Gaps. Much of the Lift 3 Area Is Rough. However, Ultrasonics Indicated That the Outlined Area Was Free From Air Gaps, Even Though it too Is Rough. Evidence of Preexisting Grout Spatters From Prior Pours Is Observed.

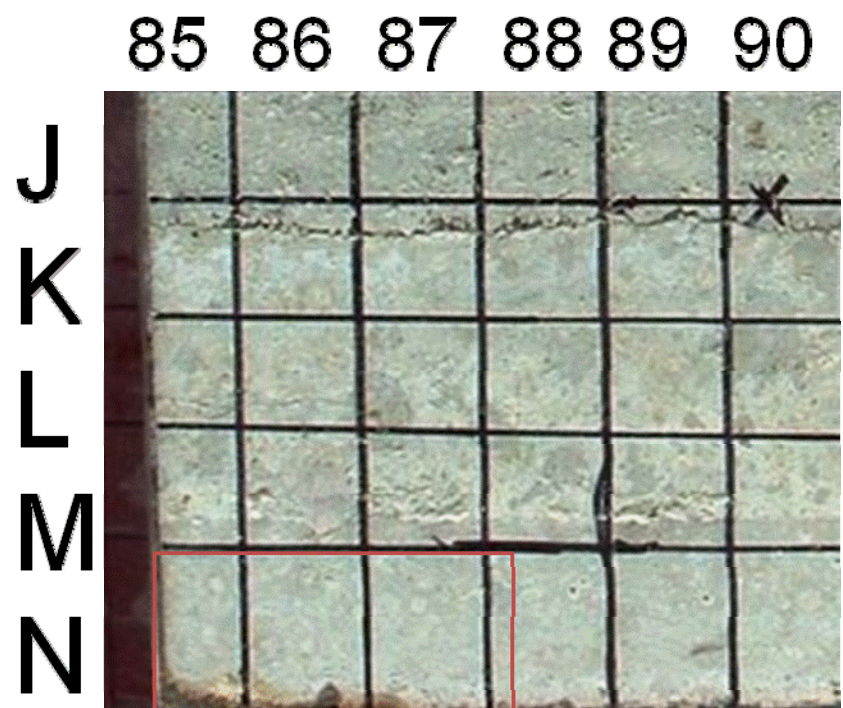


Figure 2-16. Photograph of Section Three Grout, Which Was Predicted by Ultrasonics To Have Air Gaps. Lift 1 Is Smoother Than Lifts 2 and 3, and Ultrasonics Indicated That the Outlined Area, Which Is Smooth, Was Free From Air Gaps. Evidence of Preexisting Grout Spatters From Prior Pours Is Observed Above This Level.

DSL-generated topography of the interior surface of the steel retaining wall (Figures 2-17 through 2-19).

## 2.4.2 Results and Observations

Surface roughness of the interior tank wall is produced by the relative thickness of the adhering grout material. Thickness of the adhering grout material generally ranges from a few millimeters to less than 0.1 mm [0.004 in] (Figure 2-17). Surface roughness varies with location and sometimes appears to reflect grout stratigraphy (Figures 2-17 and 2-19), although not uniformly so [Figure 2-17(a), rows D, E, and F; Figure 2-18(a), rows C, D, E, and F]. Where tank wall sections have been removed, smooth surfaces are often observed along the lower portion of a lift.

Grout appears to have variably bonded to the tank wall during curing, as indicated by observations of the interior surface of the metal tank wall, which shows that grout variably adheres to the wall. Figure 2-18(b) shows two adherence patterns corresponding to grout spatters and bulk grout pours. In the lower or subgrout portions of the interior tank wall, it appears that early grout spatters were covered during successive pours, and that in at least some cases, the spatter adheres better than the grout pour that covers it [Figure 2-19(b)]. When compared with spatters adhering to the exposed tank wall [Figure 2-18(b)], the morphology, outline, and pattern of the covered spatters are closely similar. It appears that early forming and subsequently covered grout spatter appreciably adheres to the tank wall, whereas the successive pours do not adhere as well to the tank wall or to the spatters. This may be interpreted that even where grout adheres to the tank wall, it is possible that a nonbonded contact exists within a few millimeters and parallel with the tank wall, and that this contact may intersect the grout-to-wall interface. This contact can act and appear as a crack, even though the surface or contact did not form in response to mechanical strain.

Where grout is well-bonded to the tank wall, at least some material might be expected to remain on the retaining wall when a portion of that wall is removed. Further, it is reasonable to expect that bonding between the grout body and the tank wall may hinder wall removal. During removal of the Section Three wall segment, the plate was easily pulled away from the grout. Results from the ultrasonic testing (Section 2.2) indicate that there were air gaps between the grout and the steel plate. Some difficulty was encountered while removing the plate cut from Section One. However, close examination of the saw cuts of the plate location relative to the cross-tank brace indicates that some edges were not cleanly cut prior to attempting removal. Further, when attempts were made to lever the plate from the wall, the placement and application of the leverage tended to lock the plate in position rather than pry it from the wall. It is possible that the effort required to remove the plate was more a product of the removal method than of bond strength.

Observations from DSL and photographic imagery of the interior tank wall and of the exposed grout may be interpreted to show that in some areas with little evidence of bonding, it is evident that the grout was in contact with the retaining wall in many locations. It may be that, although the grout did not adhere or bond to the tank wall, contact between the tank wall and grout was sufficient to cause some nondestructive evaluation test results to be interpreted as bonded.

## 2.5 Conclusions

Based upon comparison of the ultrasonic inspection results with the destructive testing of two sections of the intermediate-scale grout monolith's tank wall, it appears that the zero degree,

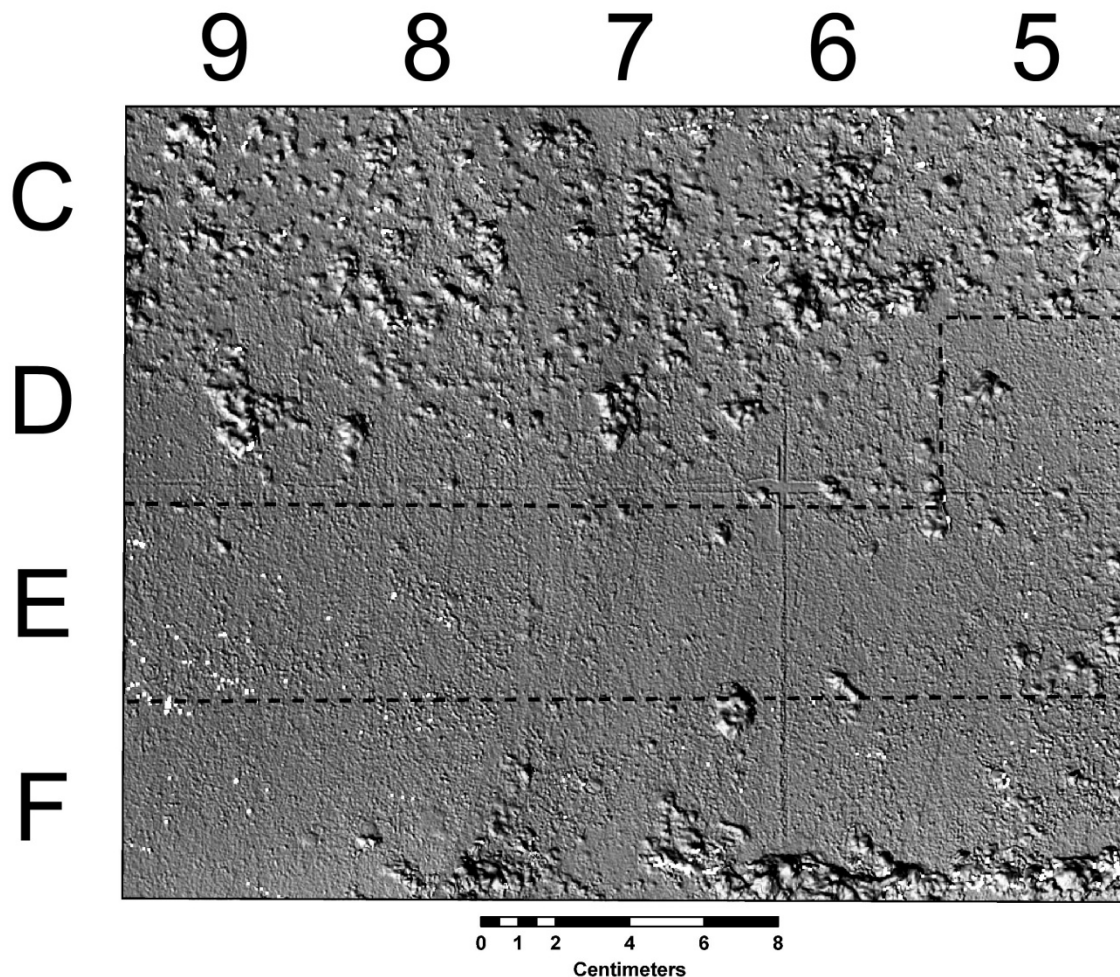


**Figure 2-17(a). Dynamic Structured Light Data, Presented as DSR of a Portion of the Upper Lift (Lift 3) Exposed on the Interior Surface of the Section One Steel Tank Wall (See Figure 2-11). Ultrasonic Testing Predicted the Relatively Smooth Area Bounded by the Dashed Lines To Have Air Gaps; Relatively Rough Areas Above and Below Were Predicted To Be Free From Air Gaps. Rough Areas Correlate to the Pitting Described in Figure 2-11. Maximum Vertical Relief of Grout Remnants Is Approximately 2 mm [0.078 in] Relative to the Surface of the Steel Plate. Observe That Column Order Is Reversed Compared With Figure 2-11; the Inner Surface of the Tank Wall Presents a Mirror Image of the Exposed Grout Wall. The Faint Horizontal (Middle of Image) and Vertical (Center Right) Linear Features Were Guidelines Lightly Drawn on the Tank Wall With Soapstone; the Intersection Is Highlighted With a Paint Marker [See Figure 2-17(b)]. The Lines Do Not Correspond to Nondestructive Evaluation Sampling Grids. Drawn Prior to Collecting DSL Data, the Marks Visible in the DSR Attest to the Method's Sensitivity.**

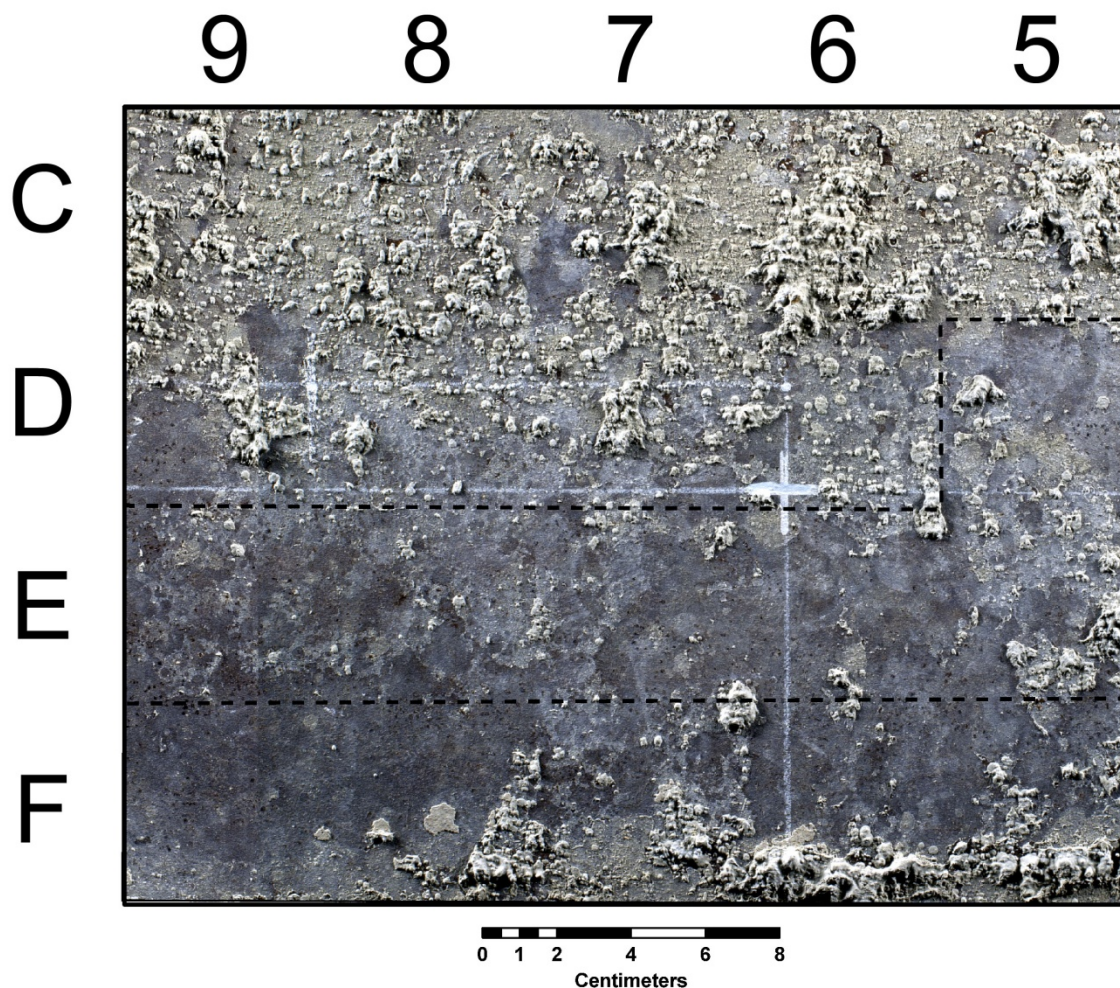


**Figure 2-17(b). Digital Photograph of the Mirror Image Area Shown in Figure 2-11 and the Area Shown in Figure 2-17(a). Area Bounded by Dashed Lines Is as In Figure 2-17a. Surface Roughness Illustrated in Figure 2-17(a) Appears as Thin Coatings of Grout  $\sim \leq 2$  mm [0.078 in] Thick That Remain Bonded to the Steel Tank Wall. Smooth Areas Appear as Grey Mottling With a Dark Red Undertone. The Grey Mottling Is Interpreted To Be a Thin Film of Grout Particles; the Dark Red Undertone Is Interpreted as the Original Antirust Red Coating of the Tank Wall and as Oxidation of the Tank Wall. Maximum Relief of the Mottled Areas Is Approximately 0.1 mm [0.039 in] Relative to the Surface of the Steel Plate.**

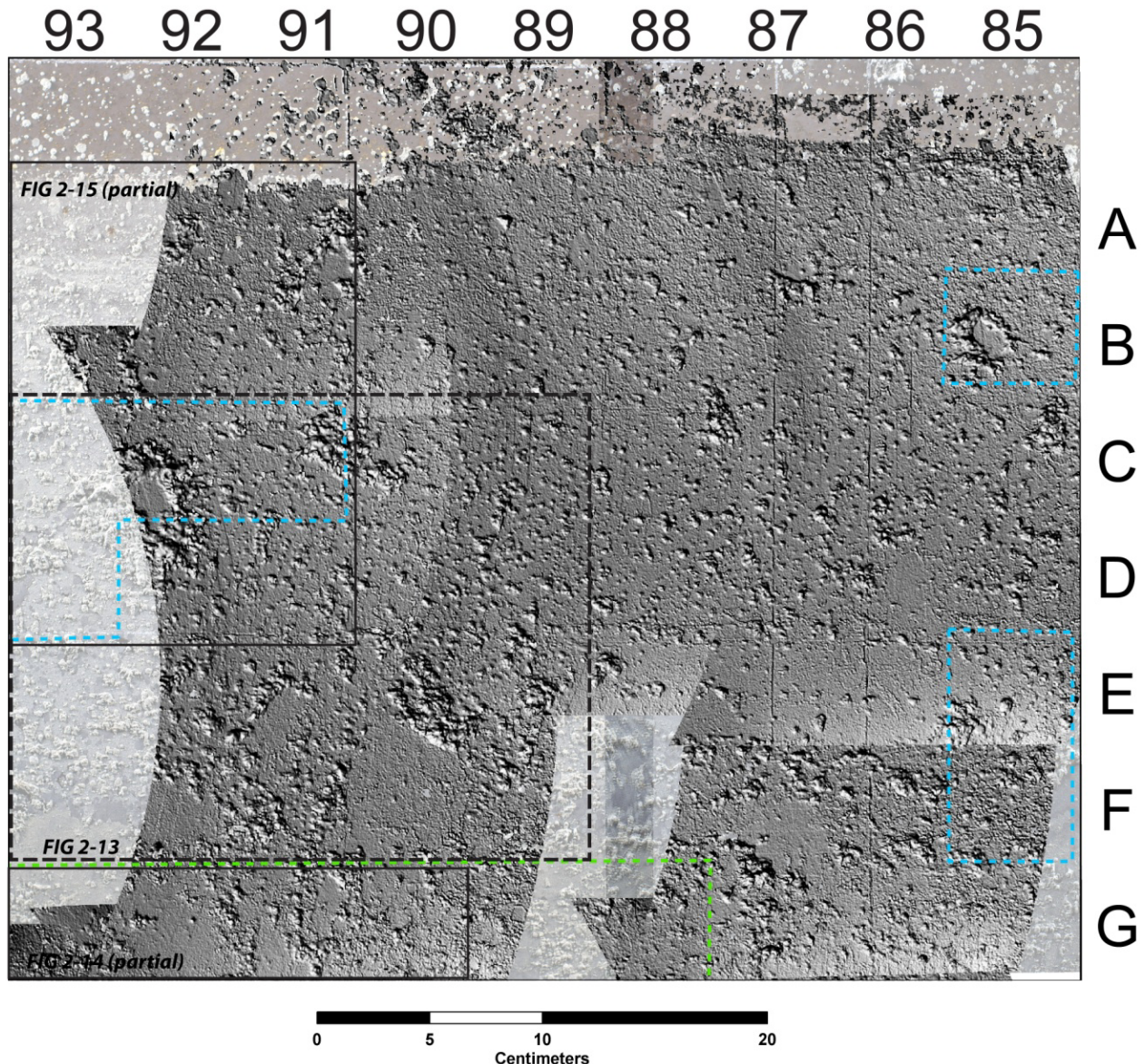


**Figure 2-18(a). DSR Mosaic of a Portion of the Interior Surface of the Section Three Wall. Areas of no Data Show a Semi-Transparent Version of the Photomosaic Shown in Figure 2-18(b). Figure 2-18(a) Incorporates the Area of Figure 2-13 (Dashed Black Line), and Portions of Figures 2-14 and 2-15 (Black Lines as Labeled). Dashed Blue Lines Encompass Areas Predicted by Ultrasonic Testing To Have Air Gaps. Dashed Green Lines Show Areas Predicted by Coin-Tap Testing To Have Air Gaps. The DSR Shows This Portion of the Tank Wall To Be Generally Rough, With Little or no Difference in Appearance Relative to Ultrasonic Testing Results. Smooth Areas Exist as Isolated Patches. Smooth Areas Appear To Be Most Common in the Lower Portion of the DSR (Rows E, F, And G). Rows A–F Show Lift 3, and Row G Shows the Uppermost Portion of Lift 2. Row G Also Contains the Only Area Predicted by the Coin-Tap Method To Have an Air Gap. The Uppermost Portion of the Image, Above Row A, Shows a Portion of the Spattered Tank Wall That Is Located Above the Surface of the Monolith [See Figure 2-18(b)].**

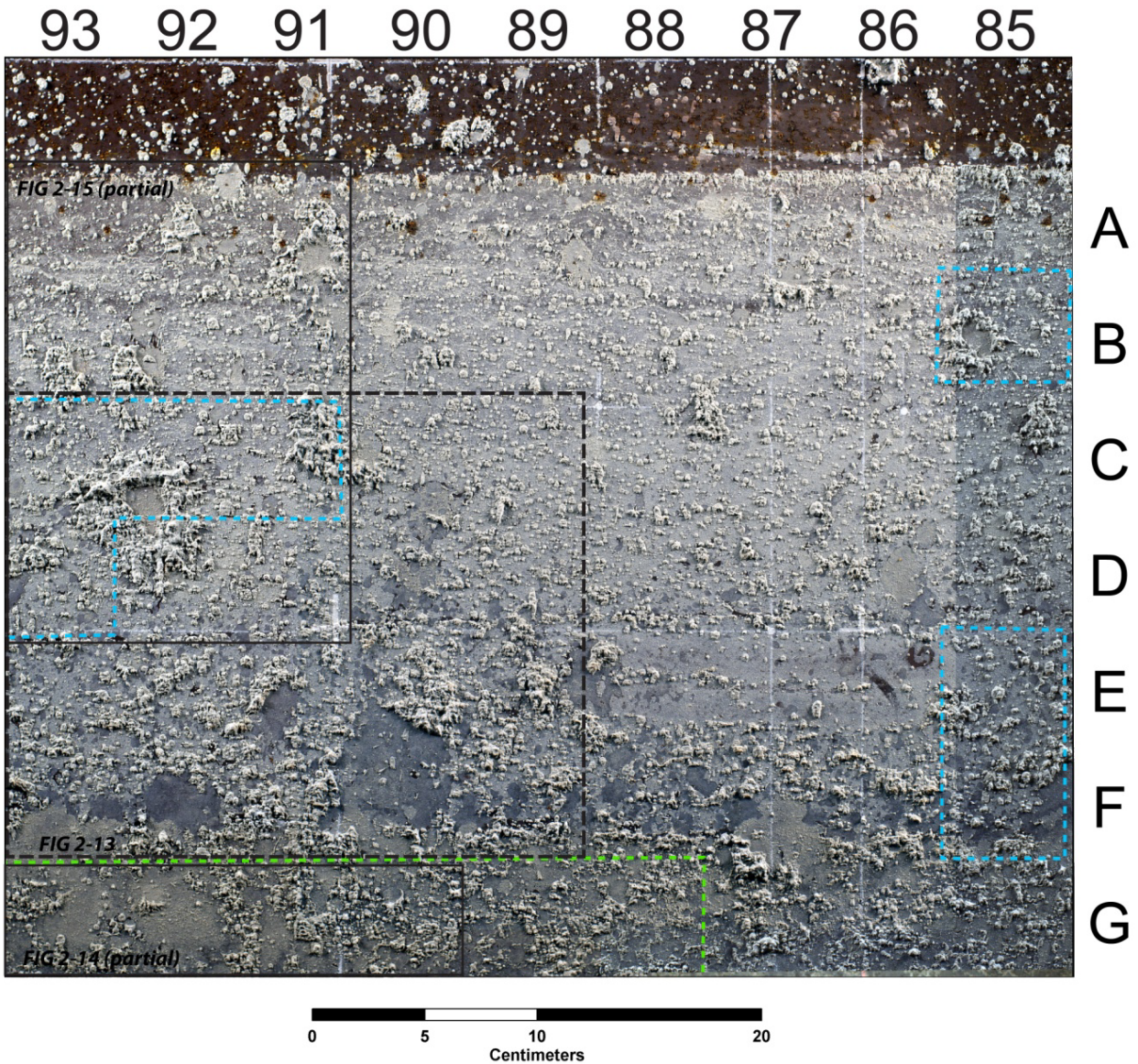


**Figure 2-18(b). Digital Photomosaic of Area Shown in Figure 2-18(a). Topographic Relief and Color Pattern Is Similar to Those Described in Figure 2-17.**

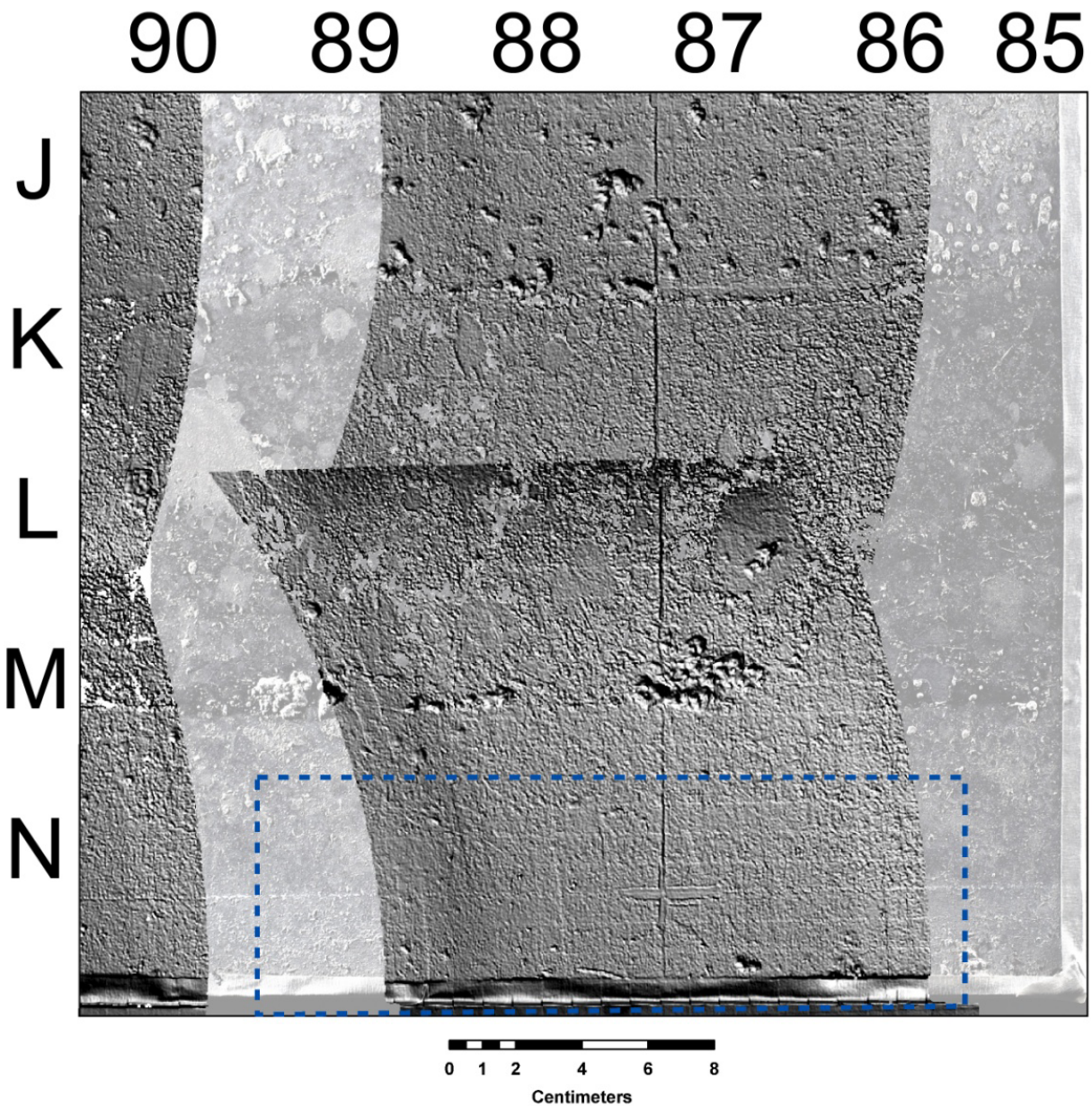


**Figure 2-19(a). DSR Mosaic of a Portion of the Interior Surface of the Section Three Steel Tank Wall, Including Portions of the Area Shown In Figure 2-16. Areas of no Data Show a Semi-Transparent Version of the Photomosaic Shown in Figure 2-19(b). The Area Within the Dashed Blue Line Is Predicted by Ultrasonic Testing To Have an Air Gap; the Remaining Area Was Predicted To Be Free From Air Gaps. The Area Is Commonly Smooth, With Rough Areas in Rows J And M. The DSR Shows the Area Predicted To Be Not Bonded (Dashed Blue Rectangle) Is Relatively Smooth, With Very Small Topographic Relief. Soapstone-Inscribed Guidelines, As Described in Figure 2-17 Are Clearly Visible.**

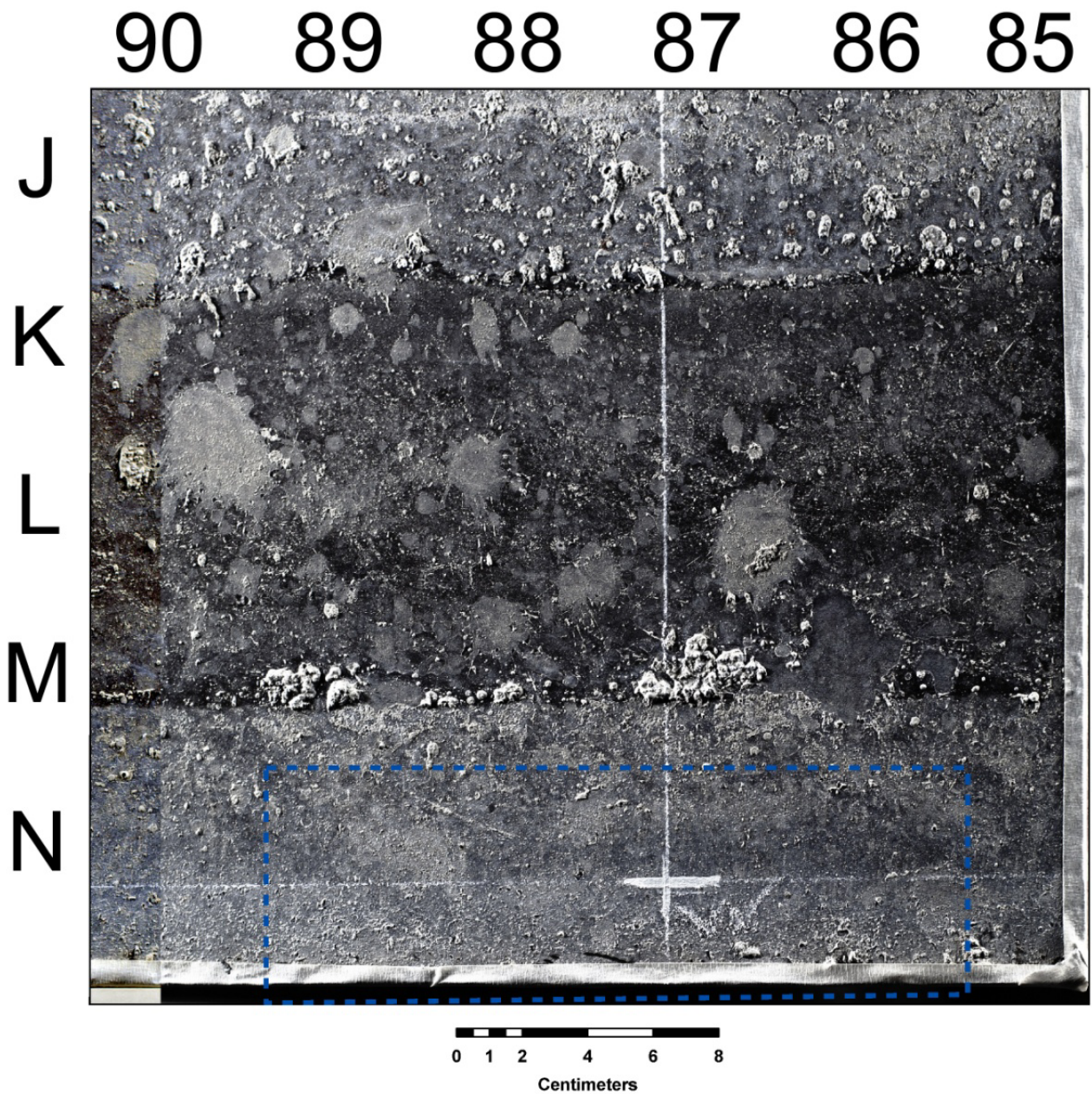


**Figure 2-19(b). Digital Photomosaic of Area Shown in Figure 2-19a. Topographic Relief and Color Pattern Is Similar to That Described in Figure 2-17. At Least Some Light-Colored Mottling Appear To Be Remnant Spatter Marks, Particularly in Rows J–M. Soapstone-Inscribed Guidelines, as Described In Figure 2-17 Are Clearly Visible.**

longitudinal ultrasonic technique provided a good means to determine whether the interface between the grout and the tank wall was affected by the presence of an air gap. While the presence of an air gap is strongly suggestive of a debonded condition, the lack of an air gap does not conclusively prove that an adequate bond exists between the grout and the tank liner or wall. Because the coin-tap test is only capable of identifying larger voids, this test method did not prove reliable for detecting small air gaps that were positively identified by the ultrasonic method, but it was useful for identifying the presence of near-surface air gaps located behind near-vertical cracks at the grout–tank wall interface (see Section 3.4 for discussion of two such cracks).

Results from DSL coupled with photographic methods give insight into the nature of the interface between tank wall and grout. Observations indicate that bonding of the grout to the tank wall is not uniform. Grout spatter sometimes adheres well to the tank wall and sometimes remains with the grout mass. Although spatter can adhere to the tank wall, the bulk grout mass that was later poured over the spatter may not adhere well to the spatter, resulting in a vertical discontinuity within a few millimeters of the tank wall. Though not a crack *sensu stricto*, the discontinuity may appear and act as would a crack.